PART - IV

CHAPTER – 9

ELECTRICAL RESISTIVITY AND OPTICAL PROPERTIES OF $InBi_{1-x}Sb_x$ AND $InBi_{1-x}Se_x$ CRYSTALS AND THIN FILMS

CHAPTER – 9

ELECTRICAL RESISTIVITY AND OPTICAL PROPERTIES OF $InBi_{1-x}Sb_x$ & $InBi_{1-x}Se_x$ CRYSTALS & THIN FILMS

This chapter reports the results obtained in the electrical and optical studies on $InBi_{1-x}Se_x$ and $InBi_{1-x}Sb_x$ (x = 0.2, 0.3, 0.4) single crystals as well as thin films. The chapter is divided into two parts. Part-A deals with the temperature dependence of electrical conductivity of the thin films variation with temperature. Part-B deals with the study of optical properties of both single crystals and thin films.

PART – A :- Electrical Resistivity :

A semiconductor is often defined to be a material with an electrical conductivity intermediate between that of an insulator and a metal. Properties of semiconductors which are generally termed as their electrical properties include [1] Electrical conductivity (or alternatively resistivity) [2] The Hall coefficient which determines the carrier density and [3] Hall mobility of the charge carriers [4] Many semiconductors change their resistance when subjected to magnetic field, the effect being known as magnetoresistivity. In this case usually the fractional change in resistivity $\Delta\rho/\rho_0$ due to applied magnetic field with respect to zero field value is obtained [5] The thermoelectric power of semiconductor is often useful. When a temperature difference is maintained between the ends of

the specimen there arises an EMF across the two ends and it is measured in $mV / {}^0C$.

Among these, the electrical resistivity is the most commonly measured property. The electrical resistivity of the vacuum deposited and heat treated thin films can give important information regarding the defect structure and density of defects present in the as-grown thin films and can throw light on the changes that take place during annealing process in the film. It is also useful to study the influence of deposition parameters on the defect density and structure of thin films by the resistivity measurements.

The Boltzmann equation is used to describe the drift of electron in an applied electric field and solution of Boltzmann transport equation leads to

$$\rho_o = mV / Ne^2\lambda \quad \ldots\ldots\ldots\ldots\ldots (1)$$

where,

m = effective mass of electron

V = Fermi velocity,

ρ_o = bulk resistivity

N = density of conduction electrons

e = charge of electron and

λ = electron mean free path.

The mean free path in a perfect rigid lattice is infinite as shown by Bloch. In other words, in a perfect lattice the electron can move without resistance. But presence of the lattice imperfections gives rise to electrical resistivity. The imperfections are of two types i.e. (1) Static & (2) Dynamic. The static defects are impurity atoms, vacancies, dislocations, grain boundaries and stacking faults. The dynamic imperfections are due to thermal motion of atoms in the lattice. The quantised vibrational modes of atoms are known as phonons.

If the temperature increases in a given lattice, the number of phonons also increases. Therefore the number of electron – phonon interactions increases as the temperature increases and the resistance also increases in turn. The temperature resistivity relation is given by

$$\rho_o = \rho_{ph[T]} + \rho_i \quad \ldots\ldots\ldots\ldots\ldots (2)$$

where, ρ_o = total resistivity, ρ_i = resistivity due to impurities, $\rho_{ph[T]}$ = Temperature dependent resistivity due to electron-phonon scattering.

Normally the dimensions of bulk conductors are several orders of magnitude larger than the mean free path of conduction electrons. Hence the total number of collisions taking place in bulk is very large compared to the number of surface collisions. However, the surface collisions cannot be neglected if one or more dimensions of the conductor approaches or are less than the mean free path, as in the case of thin films.

Polycrystalline films are made up of small single crystals in contact with one another. Except for the size, the crystallites in polycrystalline films should be similar to large single crystals. However, the effective carrier mobility is less compared to the bulk value due to additional scattering by surface. Hence the measurement of electrical properties of films should yield results which represent the average of contributions of crystallites and the grain boundaries as well as the average of anisotropies of the randomly oriented grains[1].

In the case of semiconductors, for a particular range of temperature, the density of conduction electrons increases with temperature. This is because of transition of more and more electrons from donor levels to conduction band or holes from the acceptor levels to the valence band. The energy required for this process is called the resistivity activation energy.

EXPERIMENTAL DETAILS:

Generally, Van der Pauw method is used for bulk sample resistivity. For thin films, since the resistivity is usually very high, Van der Pauw method is not practically applicable due to small values of voltage which usually cannot be measured accurately. So instead, the linear four probe method described by Goswami and Ojna[2] was used in

the present study (Fig. 1). The samples were prepared in a rectangular geometry with pre – evaporated aluminium films as the ohmic contacts (electrodes). The length to breadth ratio of the film was kept more than 4 so as to avoid geometrical influence on the electrical characteristics. The resistivity was calculated using the formula

$$\rho = \frac{RW\,a}{l} \quad \ldots\ldots\ldots\ldots\ldots (3)$$

where, ρ = electrical resistivity,

R = resistance of film,

W = breadth of film

a = thickness of film

l = length of film.

The measurement was carried out on films of different thicknesses and at different temperatures. It is known that the resistivity ρ_1 of semiconductors decreases exponentially with temperature in the intrinsic temperature range[3]. It follows the exponential relation

$$\rho = \rho_o\, e^{E\rho / KT} \quad \ldots\ldots\ldots\ldots\ldots (4)$$

where,

K = Boltzmann constant,

$E\rho$ = Resistivity activation energy.

T = absolute temperature.

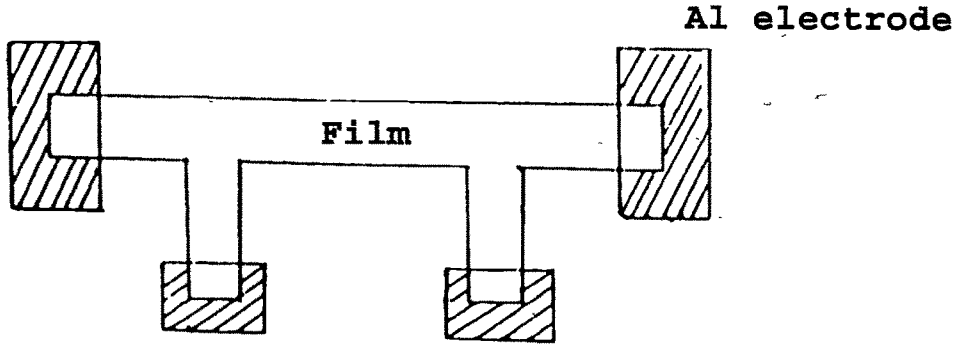

LINEAR FOUR PROBE

Fig. 1

(1) Electrical Resistivity :

Effect of film thickness: Normally, resistivity of a semiconductor decreases with increasing temperature as observed for most of the semiconductors including $InBi_{1-x}Sb_x$ and $InBi_{1-x}Se_x$. But the nature of variation is not the same for all semiconductor; it depends on whether the semiconductor is intrinsic or not, on the dopant concentration and other defects. In order to study the effect of thickness on the resistivity of the films, the films of different thicknesses were grown on glass substrates. The resistivity obtained as a function of reciprocal temperature is shown in Fig.2 and Fig. 3. The thickness was varied from 500 Å to 2000 Å at constant deposition temperature (32 ^{0}C). The resistivity measurements were carried out at different temperatures ranging from 30 ^{0}C to 80 ^{0}C using the linear four probe method. It can be seen from the plots of *l*n ρ versus l/T (Fig. 2 a, b, c, d, e and Fig. 3 a, b, c) for different thicknesses (x = 0.2), that there is nearly a linear relation following equation-4. The conductivity activation energy was calculated from the slopes of *l*n ρ versus l/T plots. Table-1 gives the observed values of conductivity activation energy for the thin films of $InBi_{1-x}Sb_x$ and $InBi_{1-x}Se_x$ of different thickness and also of compositions (similarly obtained). The average activation energy values were found to be nearly 0.05 eV and 0.045eV, for $InBi_{1-x}Sb_x$ and $InBi_{1-x}Se_x$ films, respectively. The results also indicate resistivity decreasing with film thickness. It is

$InBi_{0.8}Sb_{0.2}$ (540Å)

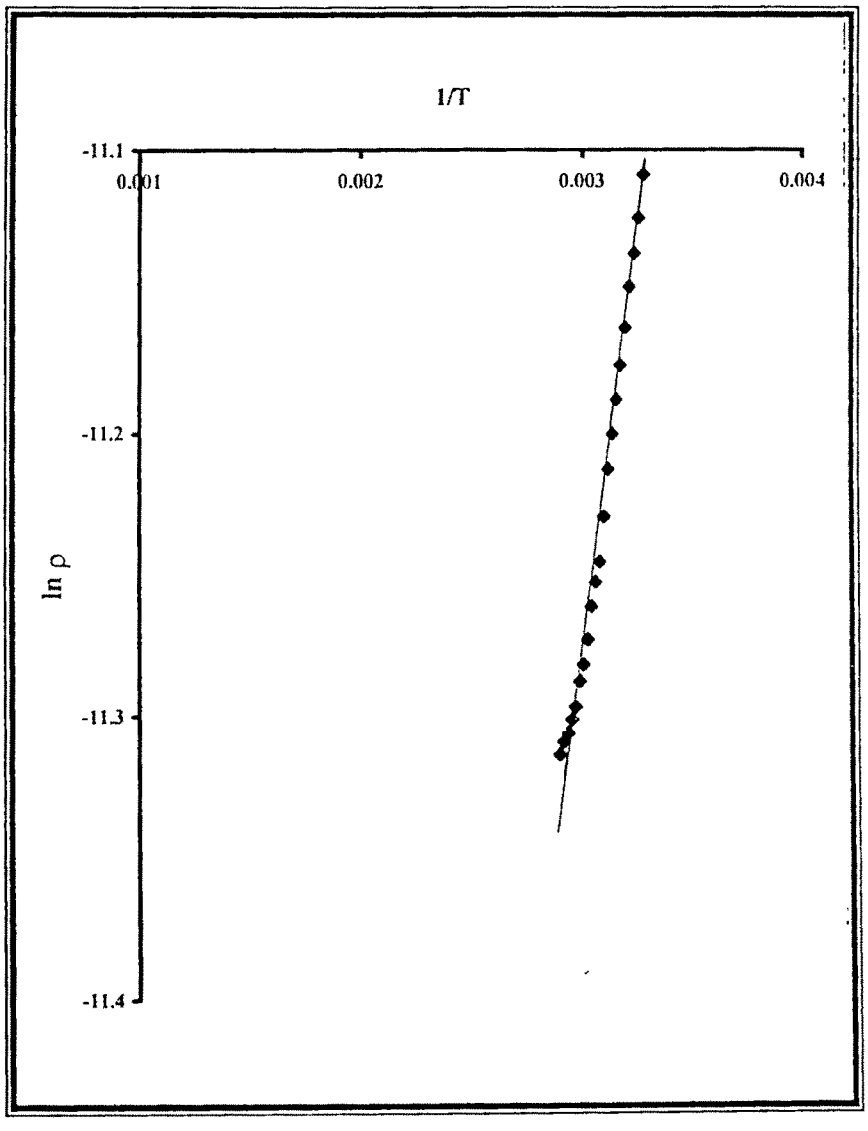

Fig. 2(a)

$InBi_{0.8}Sb_{0.2}$ (1080Å)

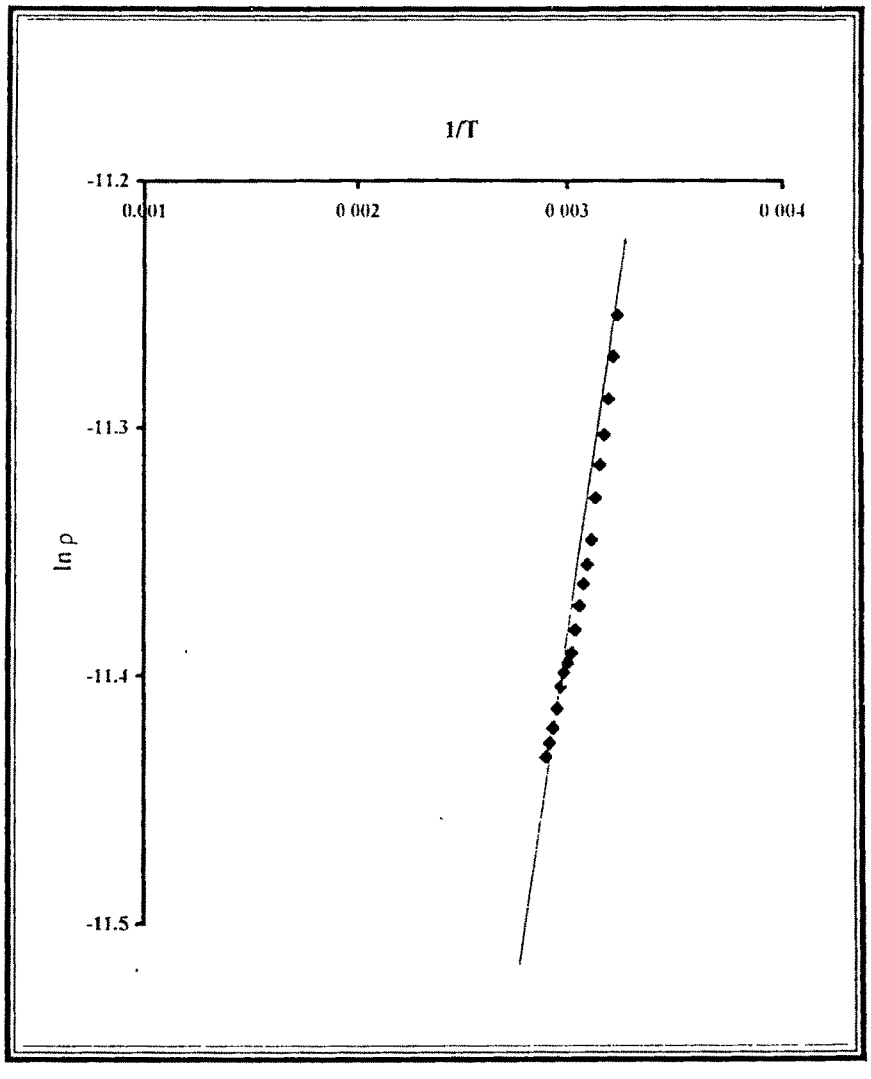

Fig. 2(b)

$InBi_{0.8}Sb_{0.2}$ (1250 Å)

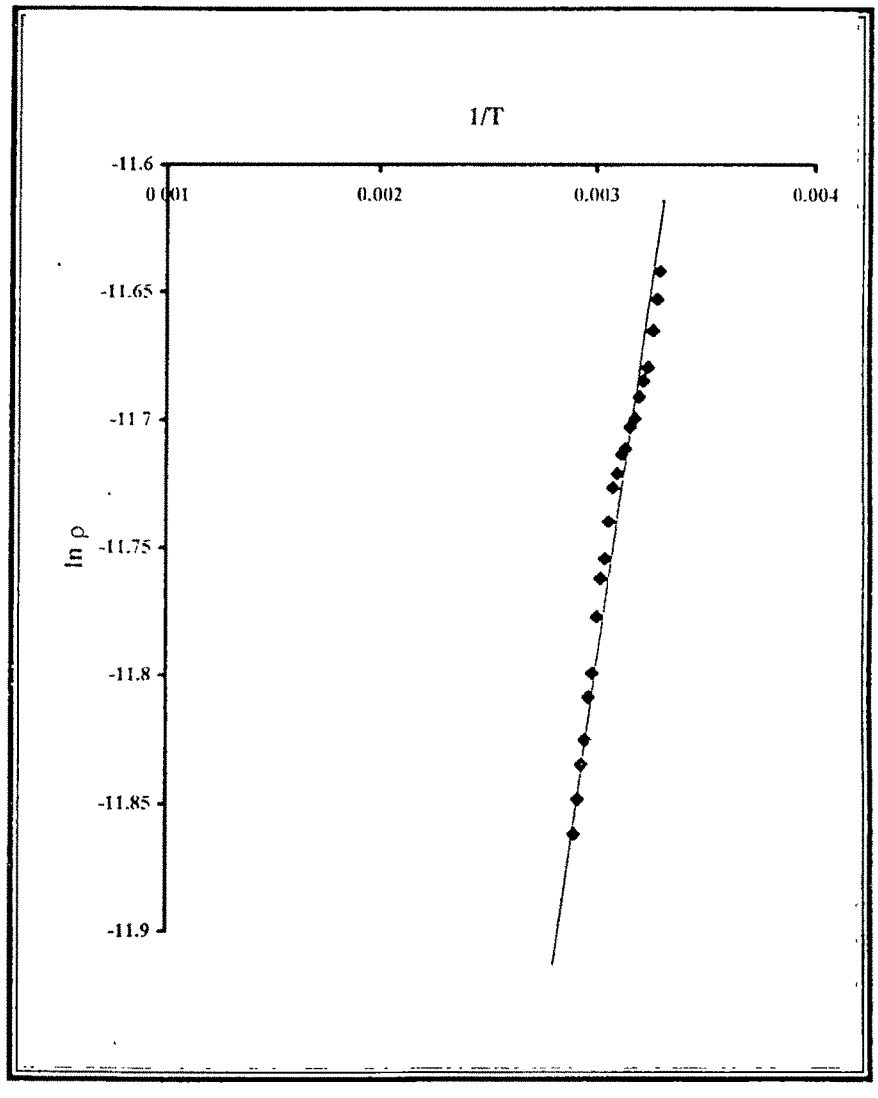

Fig. 2(c)

$InBi_{0.8}Sb_{0.2}$ (1550 Å)

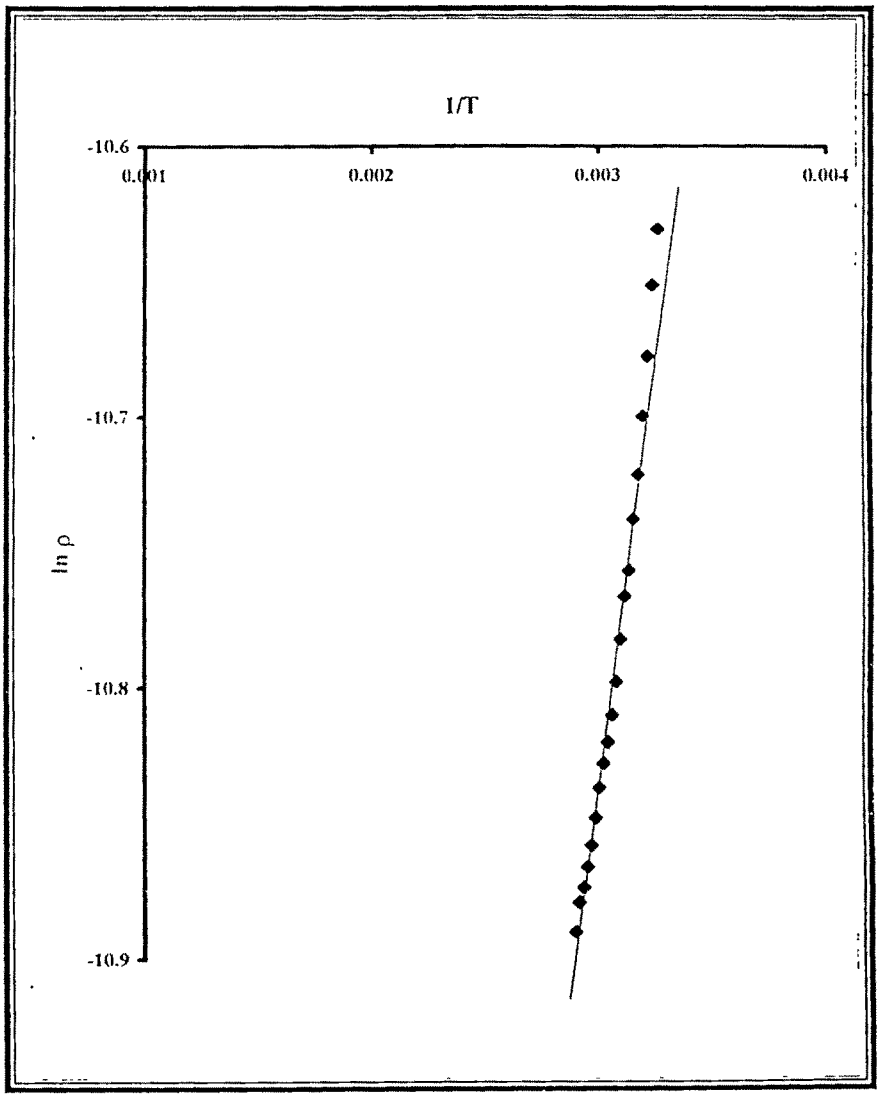

Fig. 2(d)

$InBi_{0.8}Sb_{0.2}$ (2032 Å)

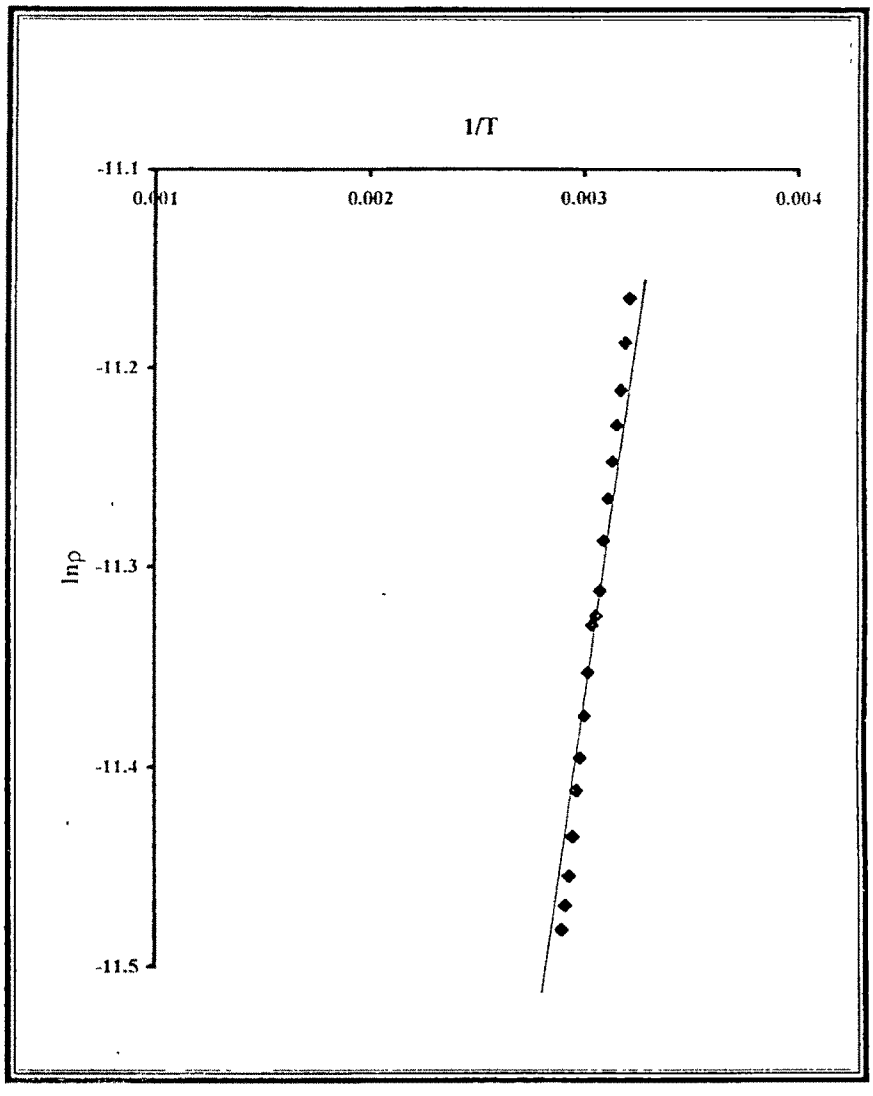

Fig. 2(e)

$InBi_{0.8}Se_{0.2}$ (1060 Å)

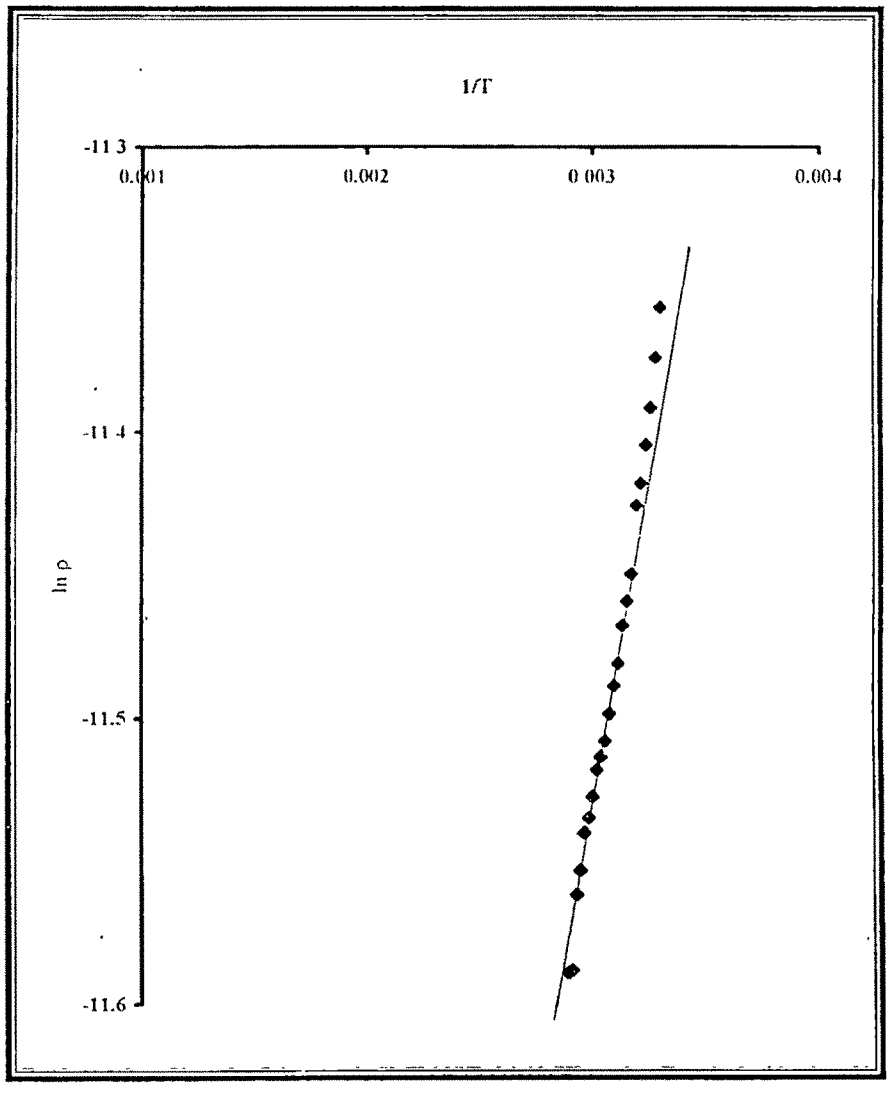

Fig.3 (a)

$InBi_{0.8}Se_{0.2}$ (1275 Å)

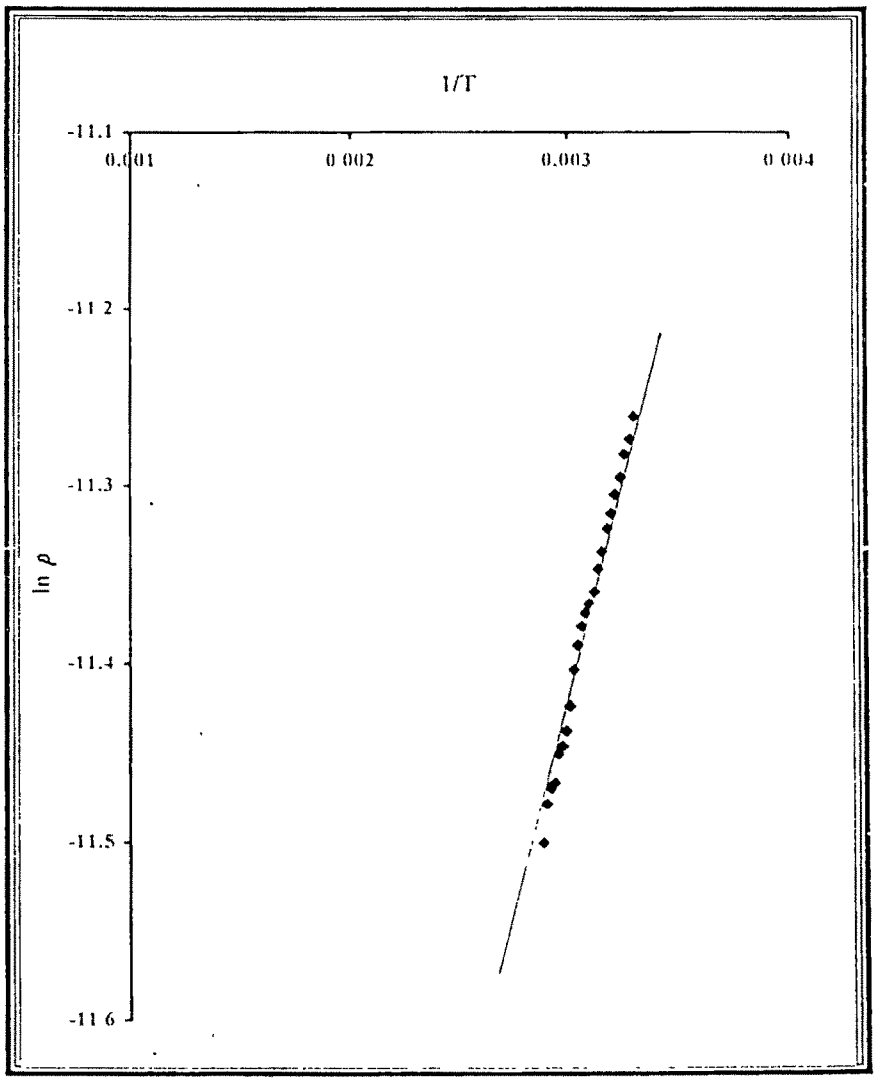

Fig.3(b)

$InBi_{0.8}Se_{0.2}$ (2032 Å)

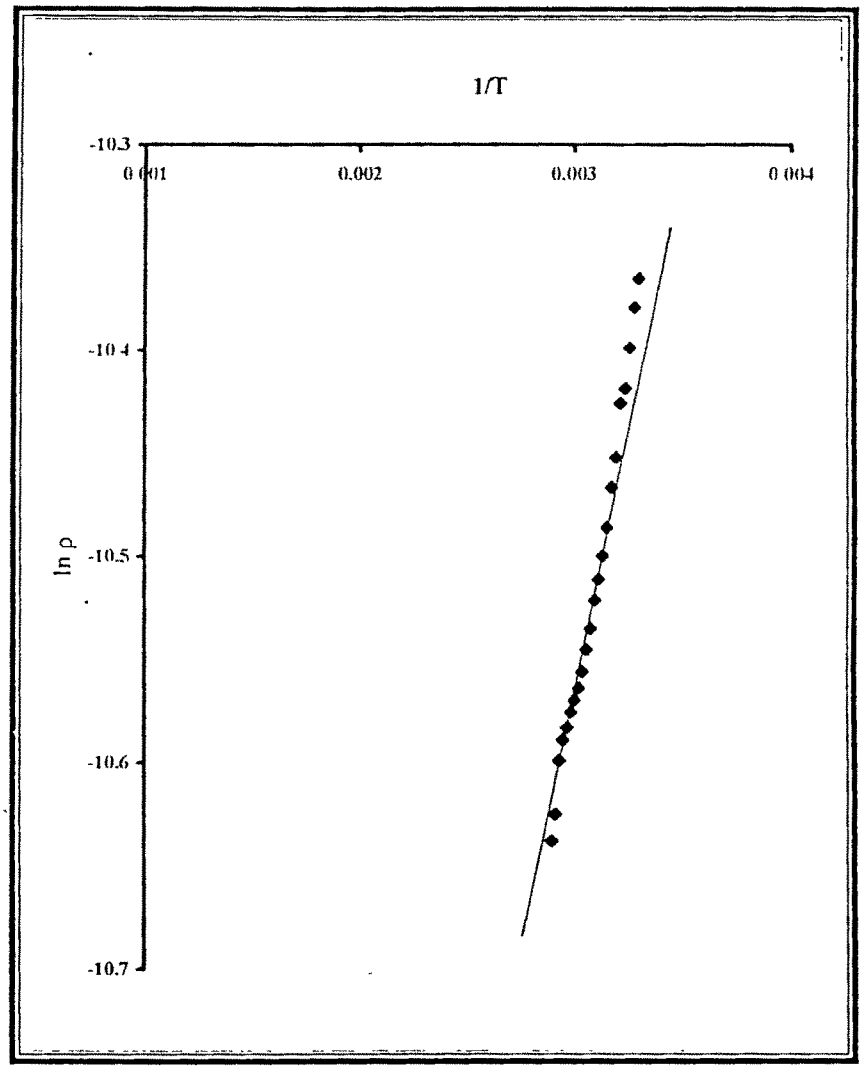

Fig. 3(c)

Table – 1

Material	Thickness (Å)	Activation energy E_ρ(eV)
$InBi_{0.8}Sb_{0.2}$	540 Å	0.051 eV
	1080 Å	0.048 eV
	1250 Å	0.049 eV
	1550 Å	0.049 eV
	2032 Å	0.056 eV
$InBi_{0.7}Sb_{0.3}$	1250 Å	0.048 eV
$InBi_{0.6}Sb_{0.4}$	1250 Å	0.047eV
$InBi_{0.8}Se_{0.2}$	1060 Å	0.039 eV
	1275 Å	0.040 eV
	2032 Å	0.049 eV
$InBi_{0.7}Se_{0.3}$	1275 Å	0.048 eV
$InBi_{0.6}Se_{0.4}$	1275 Å	0.049 eV

well known that the resistivity will respond to change in mean free path of the conduction electrons. Electron will suffer a reflection at the surface when it happens to reach it. So the resistivity increases whenever the specimen is thin enough to favour collision with the surface [to be a significant fraction of total no. of collision]. Or in other words, up to a particular thickness, with the increase in thickness the resistivity decreases[4]. Moreover, there will be an increase in size of the grains with increase in thickness. There have been reports of decreasing resistivity with increasing thickness in the case of other semiconducting thin films such as InSe[5], InTe[6], etc. The decrease in the resistivity with increase in thin film thickness is explained in terms of the films approaching bulk characteristics with increasing thickness[7].

PART – B :

Optical Band gap: The theoretical and experimental investigations of the optical behavior of solids deal primarily with optical reflection, transmission and absorption properties and their relation to the optical constants. As a result of these studies, complex multilayer optical device systems, with remarkable reflection, antireflection, interference and polarization properties have emerged for both laboratory and industrial applications. The absorption studies have led to a variety of interesting thin film optical phenomena which have thrown considerable light on the

electronic structure of solids. From reflection, transmission and absorption measurements it is possible to evaluate the optical constants such as refractive index (n), absorption index or extinction coefficient (k), absorption coefficient (α) and complex dielectric constant (ε^*) of solids. The dielectric constant also gives information about the electrical nature of the individual species constituting the solid. The study of refractive index also provides an understanding of chemical bonding and structure of the material[8 - 10]. In addition to the wide use of thin films in optical devices as mirror coatings or absorption filters, protective coatings to prevent oxidation or antireflection coatings, thin films have also been used to control the temperature of objects in outer space and as optical and thermal detectors. In all such applications, an accurate knowledge and deep sense of the optical properties of thin films are essential. Films are easier to use than bulk samples since surface roughness and lattice disorder are more easily avoided and large optically flat samples can be prepared. Very careful sample preparation techniques are required, however, if the films are to have reproducible optical properties.

The optical measurement constitutes the most important means of determining the band structure of semiconductors. For absorption studies, photons of selected wavelengths are directed at the samples and their relative transmission or absorption is measured. Optical properties of

a thin film generally differ from those of the bulk. The differences are usually attributed to the microstructure of the films.

Principally there are several methods to determine the optical constants such as Abbe's method, spectroscopic methods, polarimetric method and the critical angle method[11 - 14]. The spectroscopic method is probably the most widely used one for optical measurements. The most direct and simplest method for determining the band structure is to measure the absorption spectrum.

It is apparent that a photon with energy $h\nu \geq E_g$ can be absorbed in a semiconductor, where E_g is the band gap of the semiconductor. Since, the valence band contains many electrons and the conduction band has many empty states into the which the electrons may be excited, the probability of photon absorption is high. Fig. 4 indicates an electron excited to the conduction band by optical absorption possibly gaining more energy than is common for conduction band electrons [almost all electrons in the conduction band are near E_c unless the sample is heavily doped].

Hence an excited electron loses energy to the lattice in scattering events until its velocity reaches the thermal equilibrium velocity of the other conduction band electrons. The electrons and holes created by this absorption process are excess carriers; since, they are out of balance with their environment, they most eventually recombine. The excess carriers

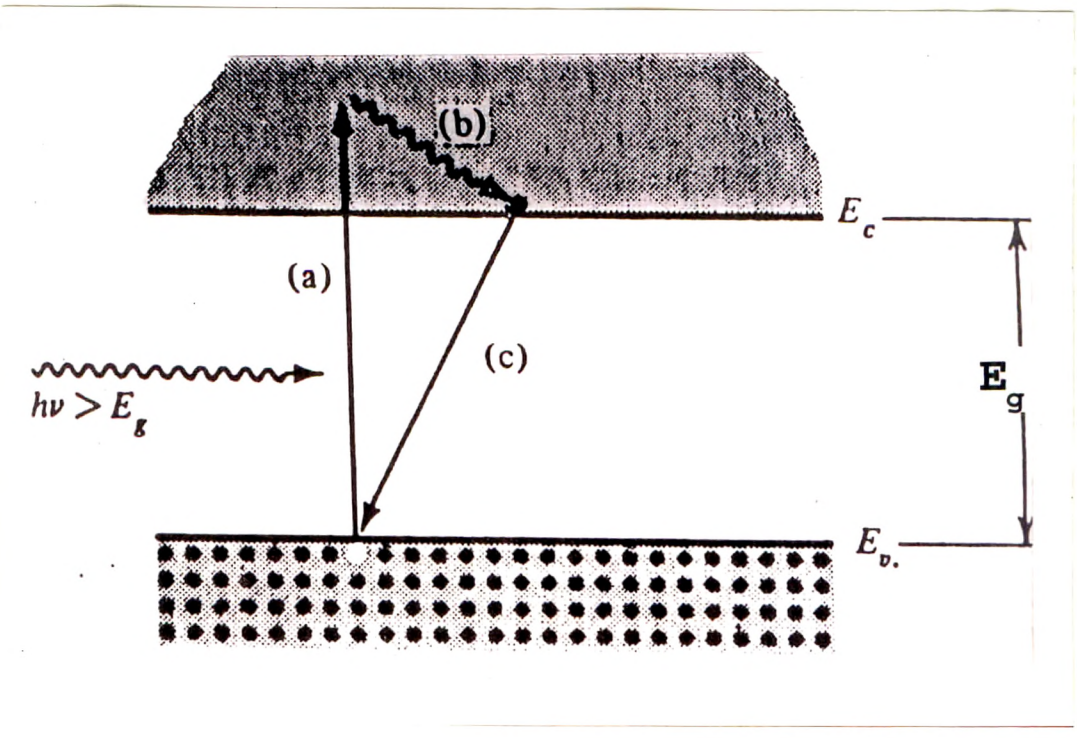

Fig. 4

exist in their respective bands. However, they are free to contribute to the conductivity of the material if not recombined.

A photon with energy less E_g is unable to excite an electron from the valence band to the conduction band. Thus, in a pure semiconductor, there is negligible absorption of photons with $h\nu < E_g$. This explains why some materials are transparent in certain wavelength ranges. Because the momentum of photon, h/λ (λ = wavelength of light) is very small compared to the crystal momentum h /a (a = lattice constant), the photon absorption process should conserve the momentum of electron. We are able to "see through" certain insulators such as an NaCl crystal, because, a large energy gap exists in this material. If the band gap is about 2 eV, only long wavelength (IR) and the red part of visible spectrum are transmitted. On the other hand, a band gap of about 3 eV allows IR and the entire visible range of spectrum to be transmitted. Band gaps of some common semiconductors relative to the optical spectrum are given in Fig. 5

Now, if a beam of photons with energy $h\nu > E_g$ falls on the semiconductor, there will be some predictable amount of absorption determined by the properties of the material. The ratio of transmitted to incident light intensity depends on the photon wavelength and thickness of the sample.

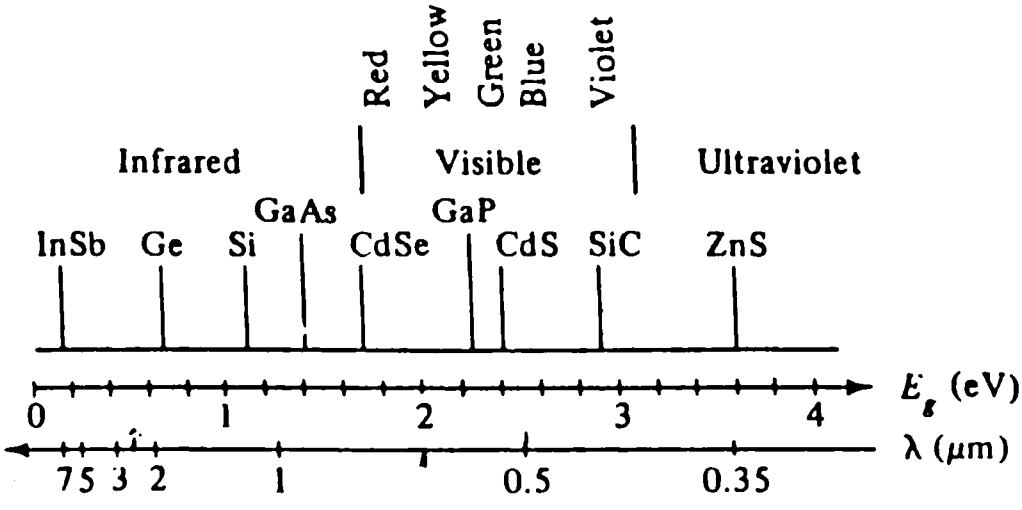
Red
Yellow
Green
Blue
Violet
Infrared
Visible
Ultraviolet
InSb
Ge
Si
GaAs
CdSe
GaP
CdS
SiC
ZnS
E_g (eV)
0
1
2
3
4
λ (μm)
7 5 3 2
1
0.5
0.35

Fig. 5

The intensity of light transmitted through the sample of thickness 't' is

$$I = I_0 e^{-\alpha t} \quad \ldots\ldots\ldots\ldots (5)$$

where, α = absorption coefficient, I_0 = incident beam intensity and I = transmitted intensity.

Near the absorption edge, the absorption coefficient can be expressed as

$$\alpha \sim (h\nu - E_g)^{\gamma} \quad \ldots\ldots\ldots\ldots (6)$$

where, $h\nu$ = photon energy, E_g = optical band gap and γ = a constant which is equal to 1/2 and 3/2 for allowed direct transition and forbidden direct transition, respectively, [with k (min) = k (max) as in the transition (a) and (b) shown in Fig. 6]. It is also equal to 2 for indirect transition [transition (c) shown in Fig.6][15], where phonons must be incorporated. In addition γ equals 1/2 for allowed indirect transitions through the exciton states where an exciton is a bound electron - hole pair with energy levels in the band gap and moving through the crystal lattice as a unit.

In the absorption process, a photon of a known energy excites an electron from a lower to a higher energy state. Thus by inserting a slab of semiconductor at the output of a monochromator and studying the changes in the transmitted radiation one can determine all the possible transitions an electron can make and learn much about the distribution of states. There are different possible transitions:

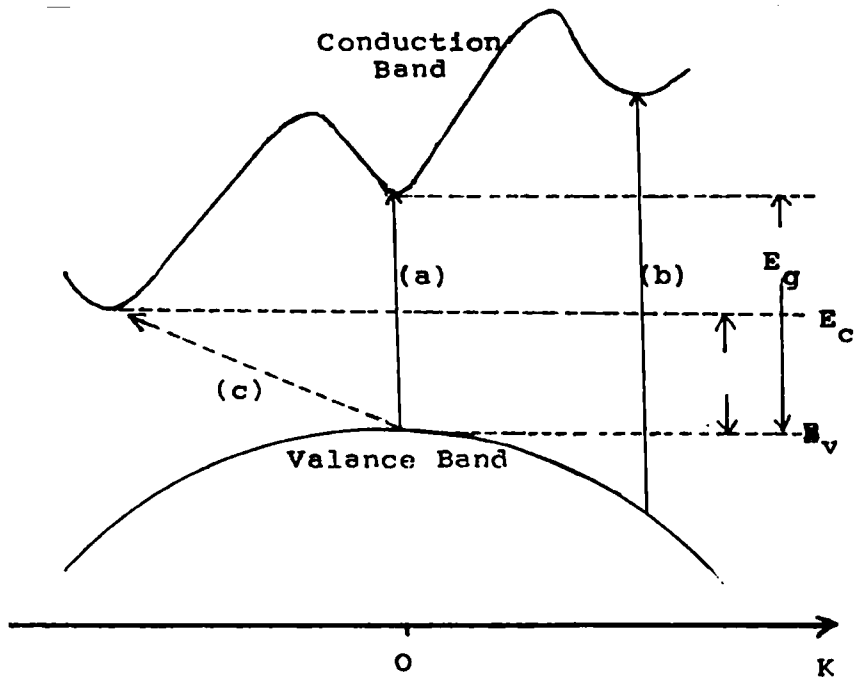

Fig. 6

(1) Band to Band (2) excitonic (3) between subbands (4) between impurities and bands (5) transition of free carriers within a band and (6) the resonances due to vibrational states of the lattice and of the impurities.

These lead to the appearance of band or absorption peaks in the absorption spectrum. Hence the spectral positions of bands determine the types of transitions occurring during the process. Absorption of light by an insulator takes place broadly by two processes

(i) by raising the electrons from valence band to conduction band.

(ii) by exciting the lattice vibrations of the material.

The latter provides information regarding bond lengths in the lattice, the effective charge on the lattice atoms and the characteristic lattice vibration frequency. From the first process, it is possible to find the electronic band structure. Thus the optical technique is a very easy way to find the band gap as compared to the electric method using the thermal excitation which is less reliable because of the fact that the effective masses of electrons and holes also influence most of the electrical parameters. The measurement of the effective mass is not very straightforward since it is coupled with many other parameters.

The absorption is expressed in terms of a co-efficient which is defined as the relative rate of decrease in light intensity L(hν) along its propagation

$$\alpha h\nu = \frac{1}{L(h\nu)} \frac{d(h\nu)}{dx} \ldots\ldots\ldots\ldots\ldots (7)$$

where, L(hν) is incident light intensity and α is absorption co-efficient [10, 16 –18]

The basic theory of direct and indirect transitions in the semiconductors is formulated by Bardeen et al[19]. The direct transitions are generally supposed to be taking place from valence band to conduction band under the selection rule,

$$K - K' + \frac{2\pi i}{\lambda} = 0 \ldots\ldots\ldots\ldots\ldots (8)$$

where, K & K' are the wave vectors of electron before and after transitions, respectively. λ is the wave length of the photon and i is the unit vector along the direction in which the photon travels before it is absorbed. This can be simplified to K = K', since $2\pi / \lambda$ is small compared to either K or K'.

This shows that only vertical transitions are allowed. Other transitions, if taking place, will be of very small probability. Thus the steep edge in absorption is attributed to the highly possible direct transitions. The weak lingering absorption in the tail part is considered to be due to indirect transitions involving the participation of phonons in the process and this will happen when the minima of the conduction band energy surface do not coincide with the maxima of the valence band

surface. A phonon is either emitted or absorbed depending on whether the energy of photon is more or less than the indirect band gap energy.

For a direct transition, the absorption coefficient relates to the photon energy as

$$(\alpha h\nu) = B (h\nu - E_g)^x \ldots\ldots\ldots\ldots (9)$$

where, x = 1/2 for allowed transitions and x = 3/2 for forbidden transitions, E_g = direct band gap energy and B is a parameter that depends on the transition probability.

For an indirect transition

$$(\alpha h\nu) = A (h\nu - E_g \pm E_p)^x \ldots\ldots\ldots\ldots (10)$$

where, x = 2 for indirect allowed transition and x = 3 for forbidden transitions, E_g = band gap and E_p is absorbed or emitted photon energy[20–22].

In actual practice, for allowed transitions, $(\alpha h\nu)^2$ is plotted against photon energy (hν) to give straight line for direct transitions [intercept on energy axis giving band gap for direct transitions] and $(\alpha h\nu)^{1/2}$ is plotted against photon energy (hν) to give a straight line for indirect transition [intercept on energy axis giving band gap for indirect transition]. Actually, two straight lines and two intercepts are usually obtained for indirect transitions; one corresponds to $E_g + E_p$ and other corresponds to $E_g - E_p$.

The lower straight line portion disappears at low temperatures. This portion corresponds to phonon absorption and no longer occurs when the population of phonon states of required energy becomes small with decreasing temperature.

The presence of excitons [usually manifested as a series of narrow absorption lines at low energy side of the intrinsic band gap absorption] appears for measurements at low temperatures only, since for most of the materials the excitons are thermally dissociated at room temperature [23].

A wide range of studies on thin films has been made using the optical measurements by various workers. For example, F.F. Sizov[24] has studied optical properties and electronic structures of IV – VI superlattice based quantum wells and has made comparison with the corresponding properties of bulk semiconductors. S.Bauer et al[25] have studied the optical properties of thin films with thickness less than the wavelength of radiation and investigated the skin depth using energy balance for incident, reflected and transmitted as well as absorbed energies. Effect of substrate structure on the optical properties of both polycrystalline and amorphous thin films have been reported by L.Bryja et al[26] in case of $Zn_3 P_2$.

Converting the semimetal InBi into a narrow band gap semiconductor by addition of Sb/Se and studying the composition

dependence of band gap have been one of the main aims of the present study. Hence the evaluation of the fundamental band gap of $InBi_{1-x}$ Sb_x and $InBi_{1-x}$ Se_x (x = 0.2, 0.3, 0.4) crystals and thin films from the absorption measurements was taken up. The absorption measurements of the samples were made on the Michelson series FTIR spectrophotometer (BOMEM, Canada). The principle of FTIR (Fourier Transform Infra Red) spectrometer possesses several advantages over dispersive spectrometers. Instead of spatially separating the optical frequencies, the FTIR spectrometer modulates all wavelengths simultaneously with distinct modulation frequencies for each wavelength. This can be done by means of variable interference effect created by separating the incoming beam into two parts and then introducing the path difference and finally recombining the beam. The resulting beam intensity is recorded as a function of optical path difference with IR detector and computing the Fourier tarnsform interferogram yields the IR spectrum (Fig 7).

In the present case, the KBr pressed disk technique was used because of its simplicity and its ability to produce good spectra from very small samples. Further using KBr as a matrix has following advantages:

(1) High transmission of radiation

(2) Chemical stability

(3) High purity

(4) Low sintering pressure.

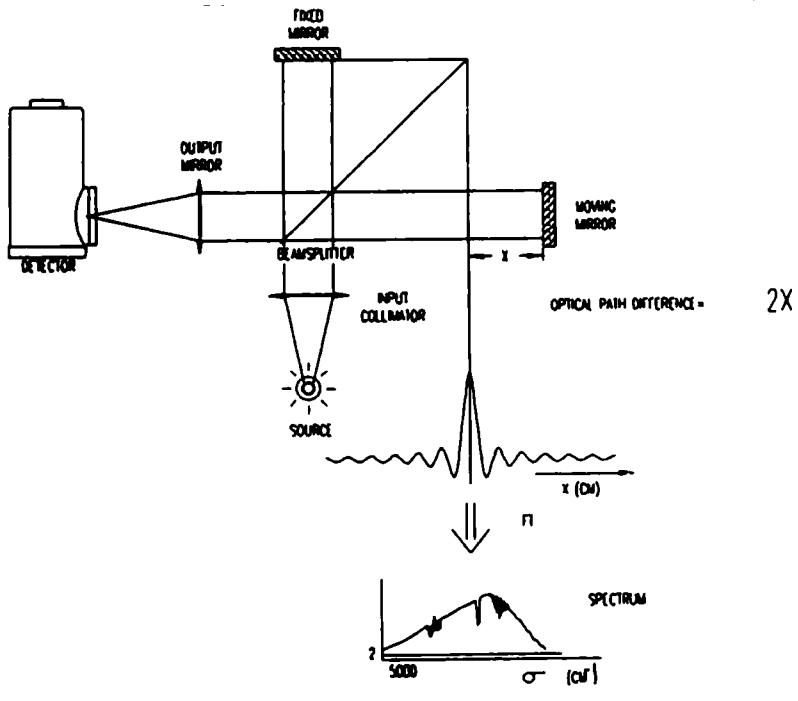
FIXED MIRROR
OUTPUT MIRROR
DETECTOR
BEAMSPLITTER
MOVING MIRROR
X
INPUT COLLIMATOR
OPTICAL PATH DIFFERENCE = 2X
SOURCE
x (CM)
FT
SPECTRUM
2
5000
σ (CM⁻¹)

Fig. 7

The crystalline powder sample (20 mg) and spectroscopic grade KBr (dry) powder matrix (350 mg) was ground to a very small particle size (few μm) and was mixed thoroughly. Then it was transferred to a die of about 1 cm diameter and evacuated at 10^{-2} torr for at least 5 min. Then a pressure of about 1.5 ton was applied for 5 min and then vacuum was released. This gives the mixture formed into a pellet. The pelletted samples were used to obtain the absorption data which were used to study the optical band gap.

The optical absorption was measured in the wave number range 510 cm^{-1} to 4000 cm^{-1} and the absorption spectrum was recorded. By analyzing the spectrum, absorption coefficient was calculated as a function of the photon energy. Since in the case of pelletted samples the thickness of the material is undetermined, an arbitrary thickness was assumed. Of course this would not give absolute absorption coefficient. However, the relative variations only are significant for the purpose of evaluating the band gap. Similarly for the thin film studies, the film was deposited on an NaCl crystal as a substrate and then absorption data was taken.

Optical Band Gap of the $InBi_{1-x}Sb_x$ / Se_x Crystals :

The plots of $(\alpha h\nu)^2$ versus $h\nu$, where $h\nu$ is the photon energy were obtained for samples as described above. The plots are shown in

Fig. 8, 9,10 for $InBi_{1-x}$ Sb_x and Fig.11, 12, 13 for $InBi_{1-x}$ Se_x, respectively for different x. The extrapolation of the straight line on the higher energy side to $(\alpha h\nu)^2 = 0$ gives the band gap values that are listed in Table 2. In both the psuedobinary systems, the band gap increases with increasing the concentration of the impurity. Thus the addition of Sb / Se as impurity in InBi is found to convert InBi into a semiconductor. The conversion has also been reported by other workers through Mossobauer / conductivity studies[27]. Also, the variation of Sb /Se concentration changes the band gap as observed.

The results indicate that the semi-metal InBi converts to semiconductor upon addition of Sb/Se. Both these elements form equilibrium phases with In, namely InSb and InSe. Hence it is likely that Sb and Se substitute Bi in $InBi_{1-x}Sb_x$ / Se_x. The compounds InSb and InSe are known to be semiconductors. The addition of Se or Sb into InBi may result into a considerable contribution of co-valent bond. The conductivity results discussed earlier also confirm the transition of InBi from semi-metallic state to semi conducting state upon addition of Sb/Se.

Optical band gap of $InBi_{1-x}Sb_x/Se_x$ thin films:

To carry out the absorption measurements on the thin films, the films were deposited on NaCl crystal substrates and were placed in the sample compartment of the IR spectrophotometer. The absorbance was

$InBi_{0.8}Sb_{0.2}$

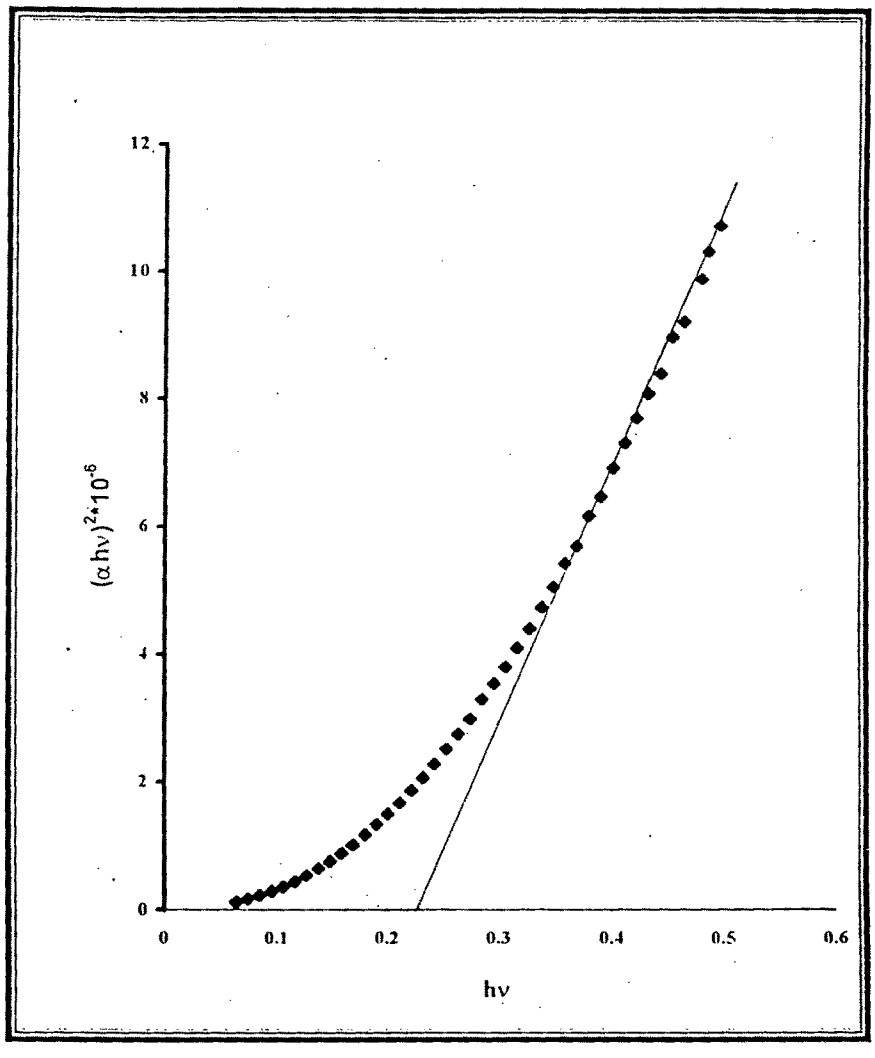

Fig. 8

$InBi_{0.7}Sb_{0.3}$

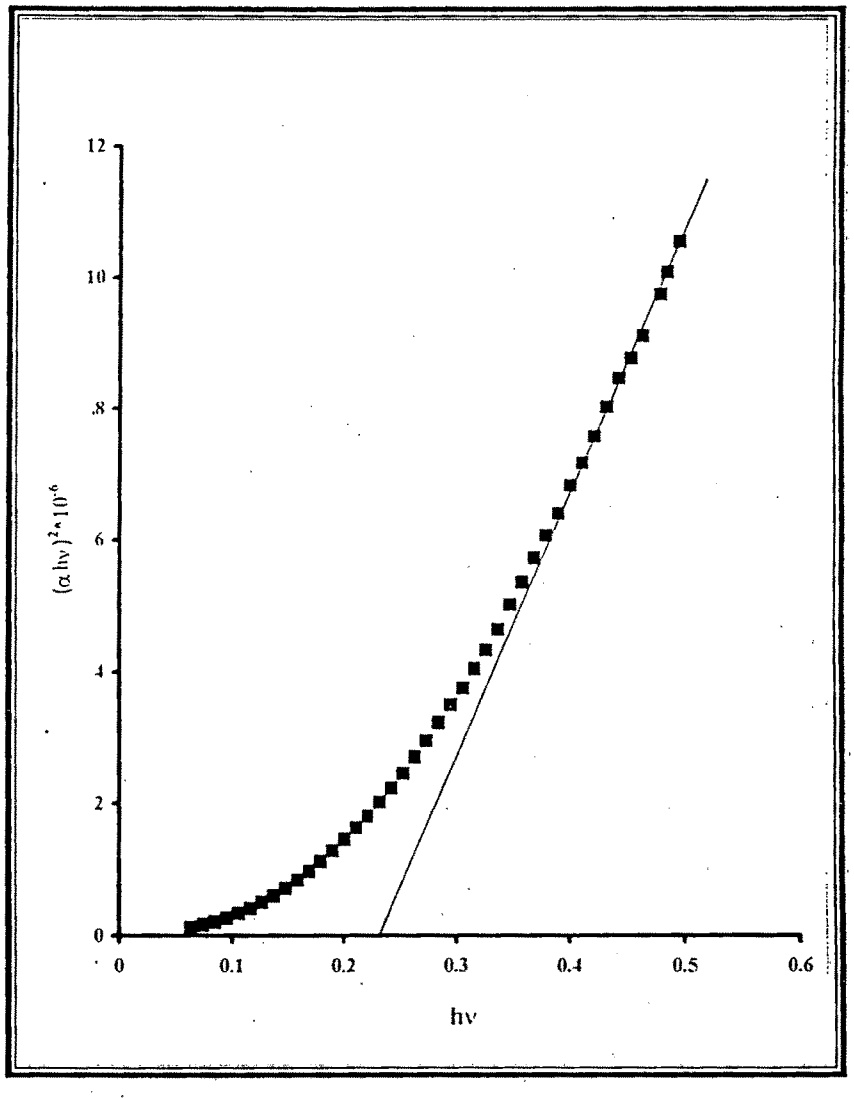

Fig. 9

$InBi_{0.6}Sb_{0.4}$

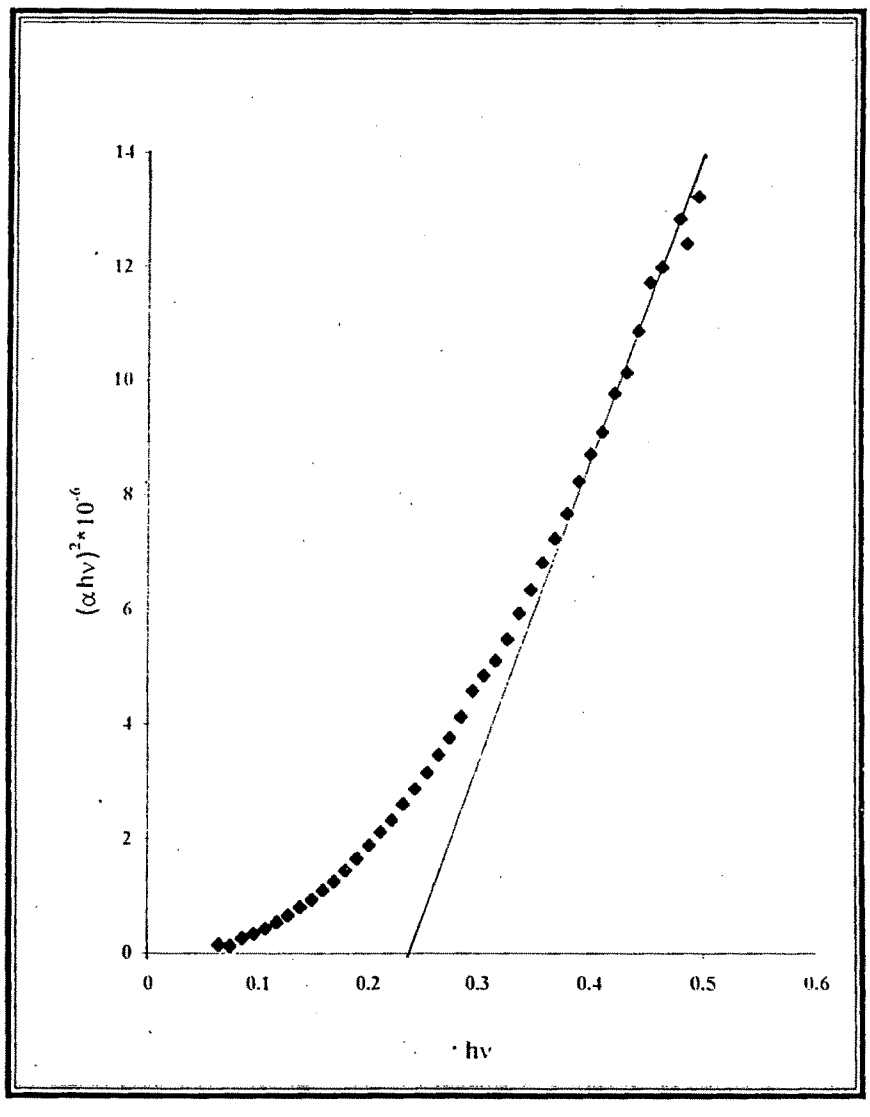

Fig. 10

$InBi_{0.8}Se_{0.2}$

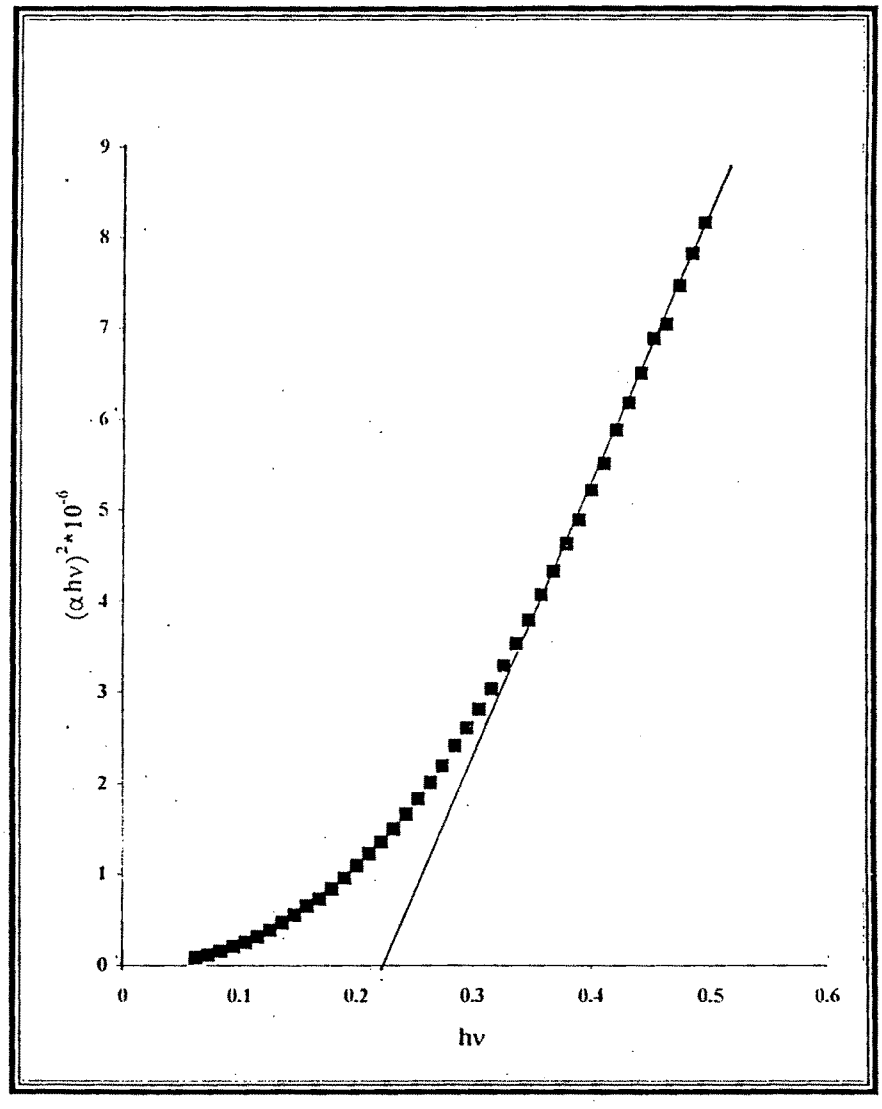

Fig. 11

$InBi_{0.7}Se_{0.3}$

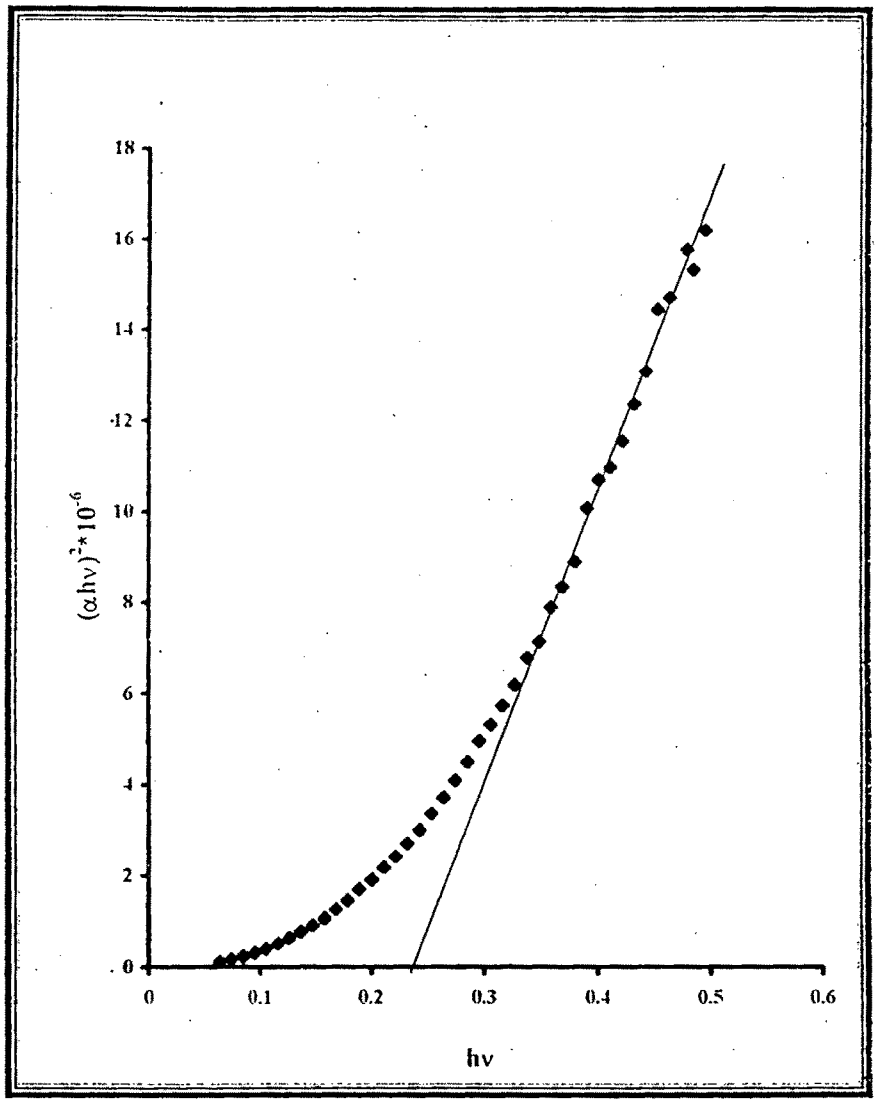

Fig. 12

$InBi_{0.6}Se_{0.4}$

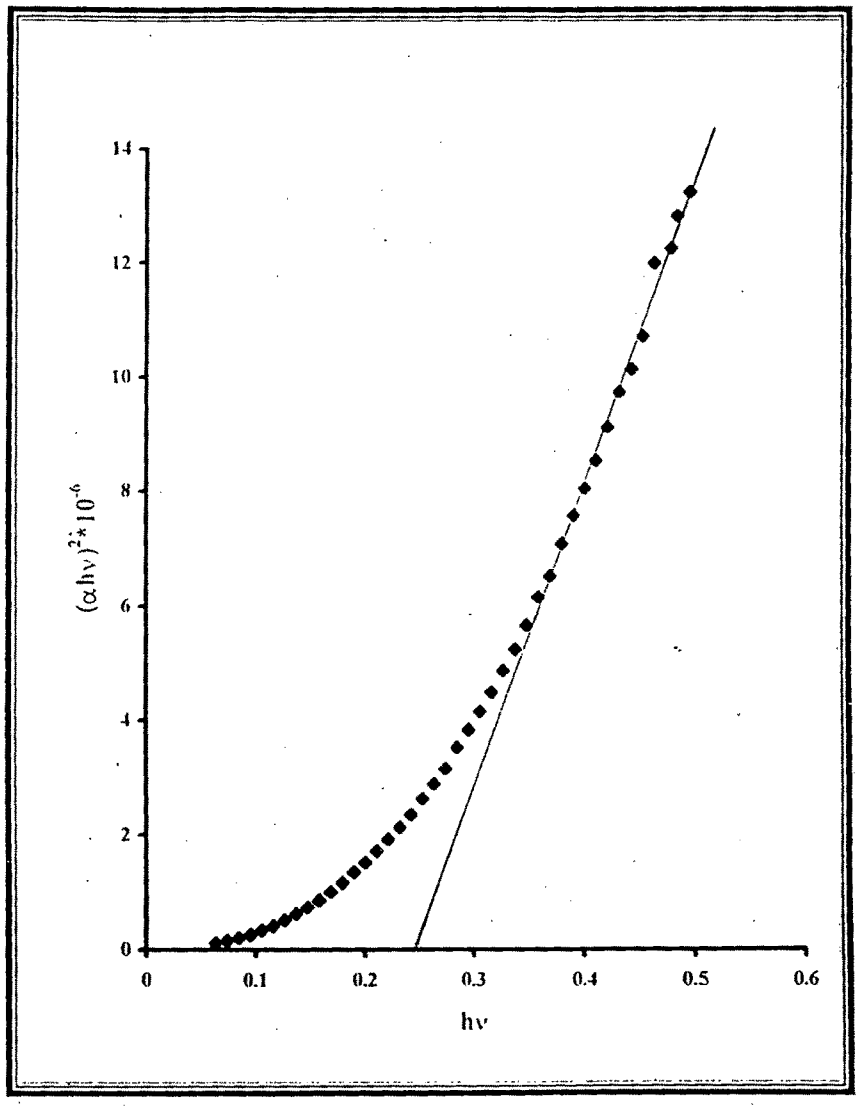

Fig. 13

Table – 2

Material	Optical band gap in eV
$InBi_{0.8}Sb_{0.2}$	0.226
$InBi_{0.7}Sb_{0.3}$	0.231
$InBi_{0.6}Sb_{0.4}$	0.236
$InBi_{0.8}Se_{0.2}$	0.225
$InBi_{0.7}Se_{0.3}$	0.237
$InBi_{0.6}Se_{0.4}$	0.250

measured in the wave number range 510 cm^{-1} to 6000 cm^{-1}. The data was used to obtained the band gap. The band gap was found to depend on the film thickness and also on the content of Se and Sb.

The plots of $(\alpha h\nu)^2$ versus $h\nu$ obtained for films $InBi_{1-x}Sb_x$ and $InBi_{1-x}$ Se_x (x = 0.2) (of different thicknesses) prepared by thermal evaporation of the compounds are given in Fig.14 (a), (b), (c), (d), (e) and Fig 15 (a), (b), (c). The plots are observed to be straight lines in the region of high absorption. Hence by extrapolating the linear portion to $h\nu = 0$ (zero abscissa), the band gap was evaluated[17, 28, 29]

The optical band gap 'Eg' plotted versus inverse square of film thicknesses (t) is shown in Fig 16 (a) & (b), respectively for $InBi_{0.8}Sb_{0.2}$ and $InBi_{0.8}Se_{0.2}$ films. Such thickness dependence of band gap has been explained in terms of quantum size effect and dislocation density. In semi metals and semiconductors, the quantum size appears when their film thicknesses is comparable with or less than the mean free path or effective de Broglie wavelength of carriers. Because of the small thickness of the films, the transverse component of quasi momentum of carriers is quantised and it assumes discrete values along the thickness dimension. The energy spectrum represents a system of the discrete levels with the separation between them given by the uncertainty principle. Due to this quantization, the bottom of the conduction band and the top of the valence

$InBi_{0.8}Sb_{0.2}$ (540 Å)

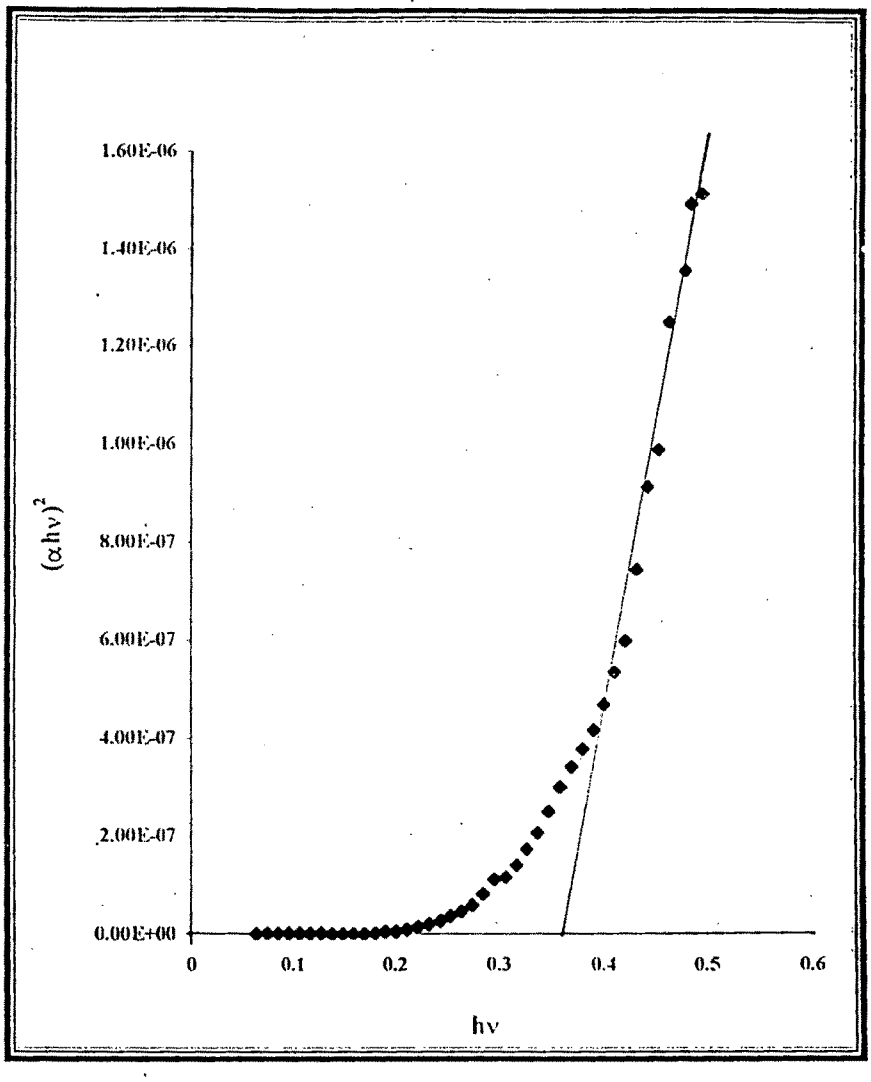

Fig. 14 (a)

$InBi_{0.8}Sb_{0.2}$ (1080 Å)

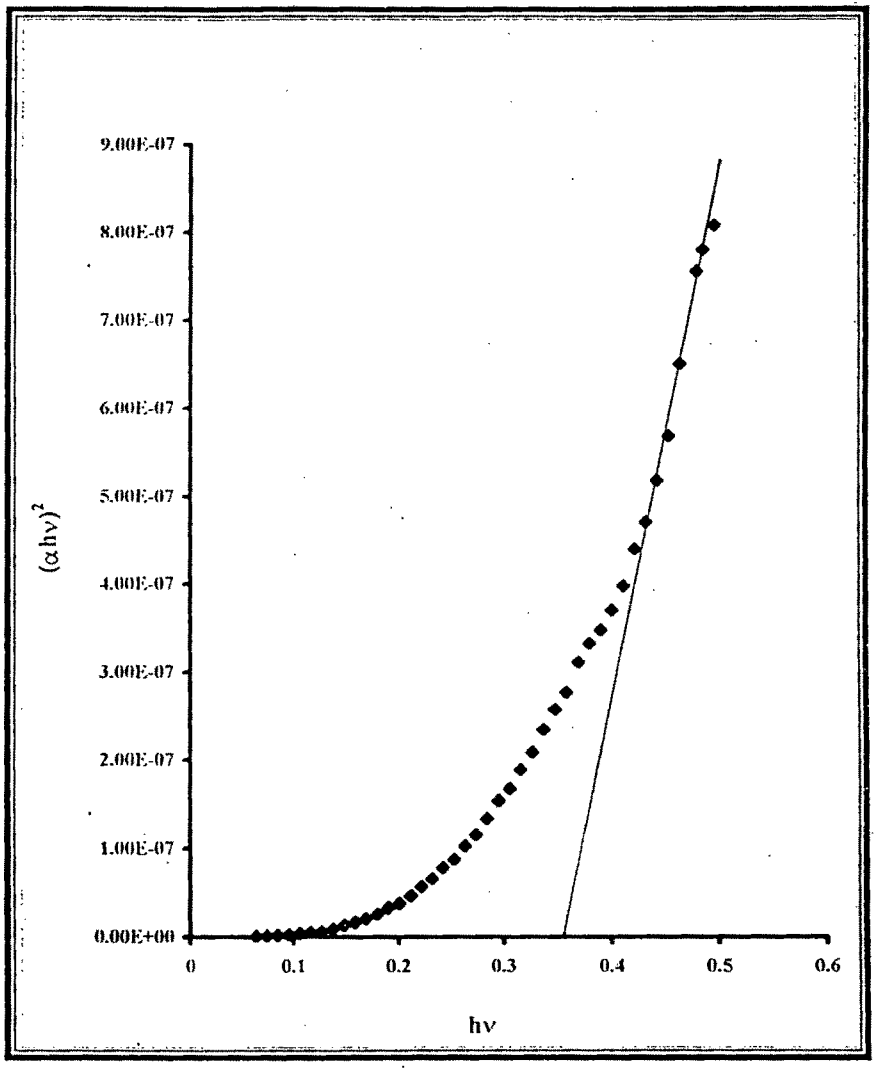

Fig. 14(b)

$InBi_{0.8}Sb_{0.2}$ (1250 Å)

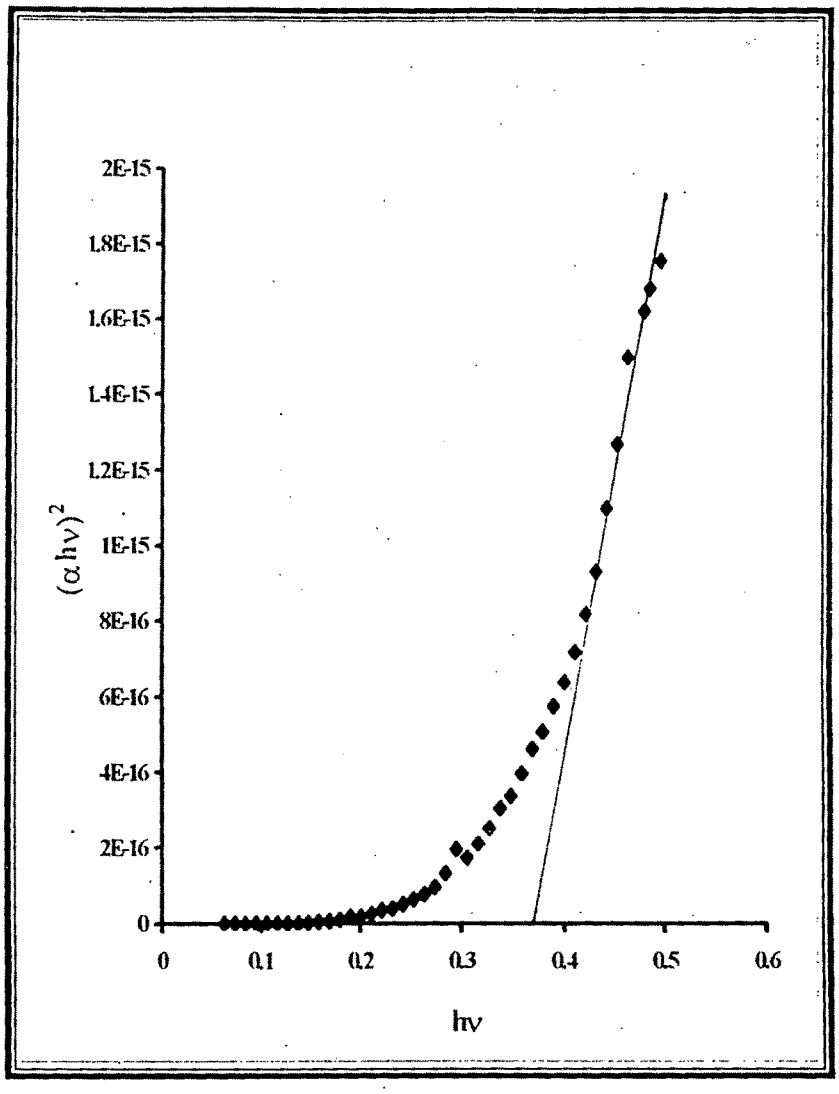

Fig. 14(c)

$InBi_{0.8}Sb_{0.2}$ (1550Å)

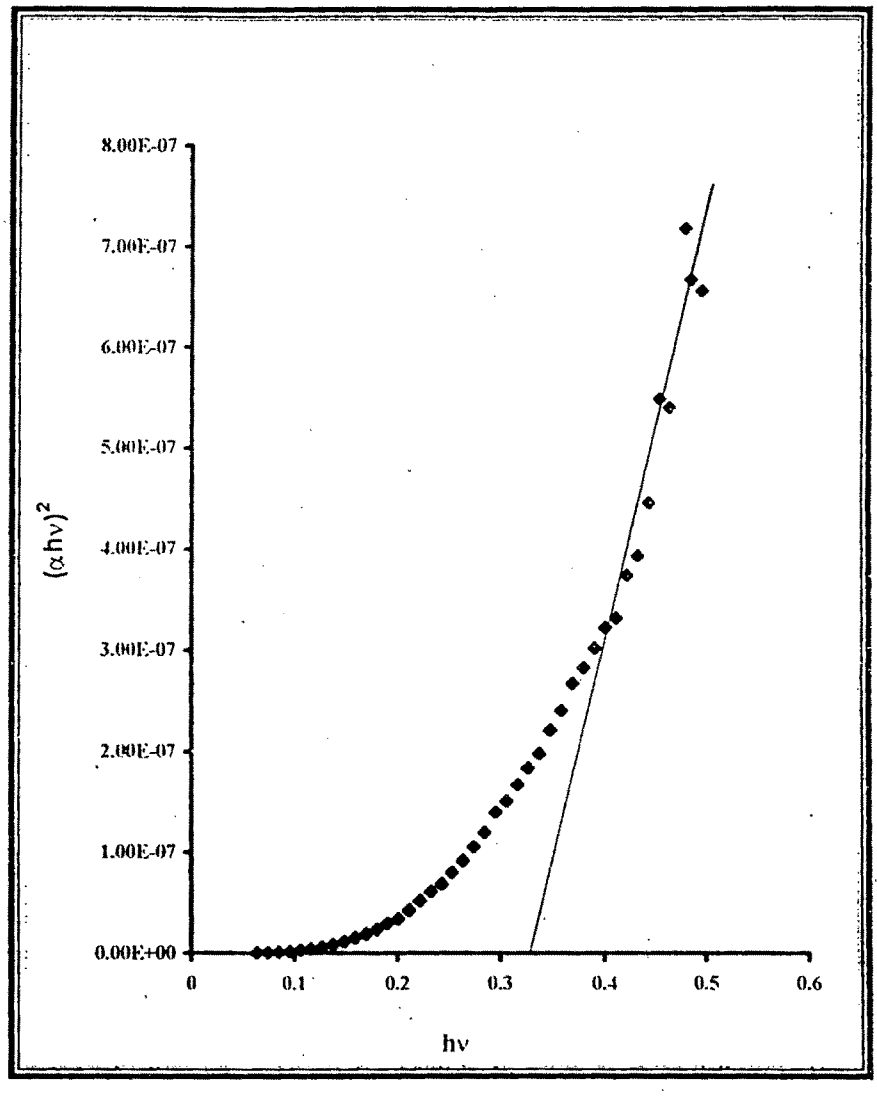

Fig. 14(d)

$InBi_{0.8}Sb_{0.2}$ (2032 Å)

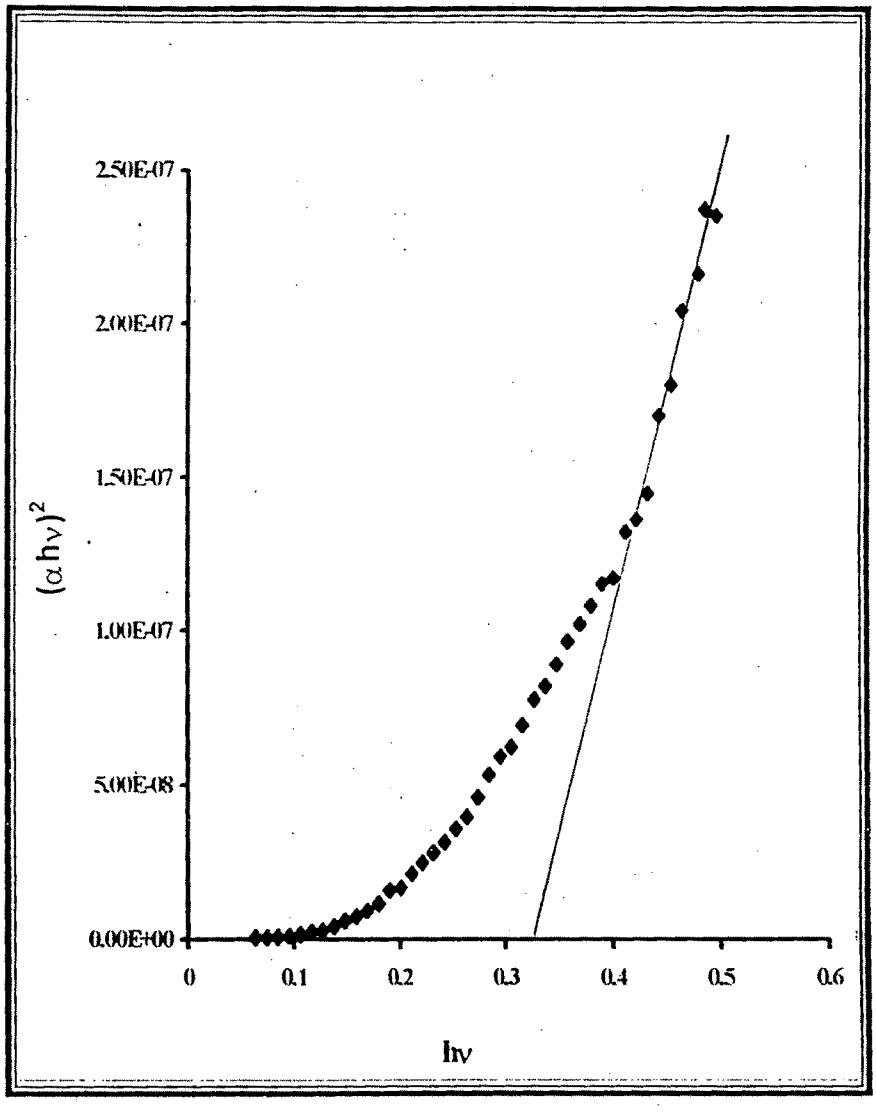

Fig. 14 (e)

$InBi_{0.8}Se_{0.2}$ (1060 Å)

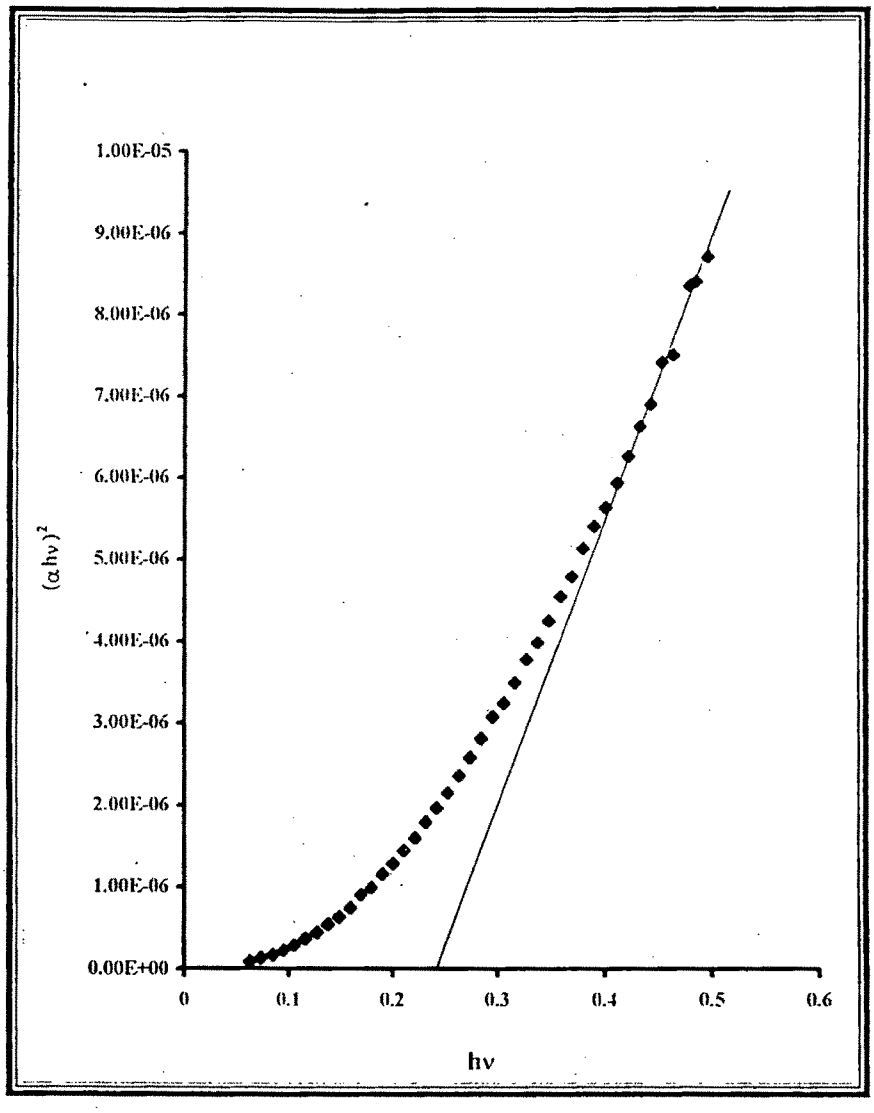

Fig. 15(a)

$InBi_{0.8}Se_{0.2}$ (1275Å)

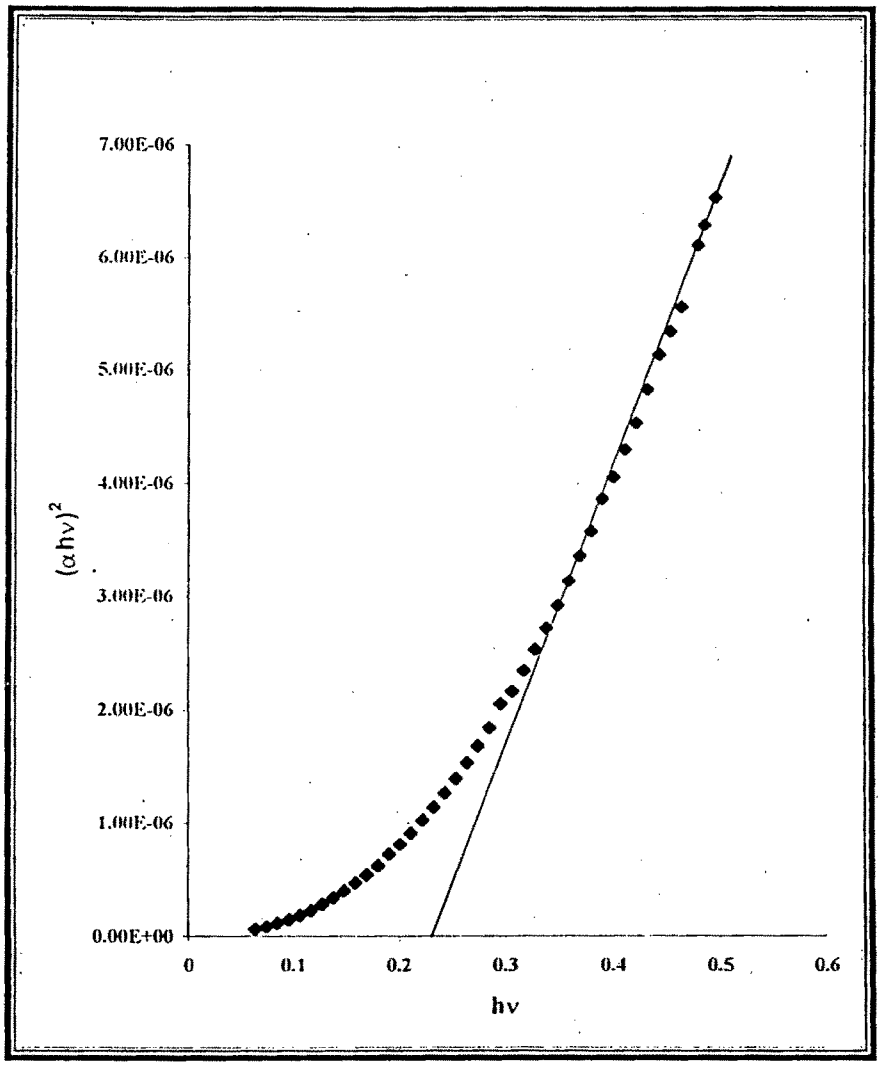

Fig. 15(b)

$InBi_{0.8}Se_{0.2}$ (1502Å)

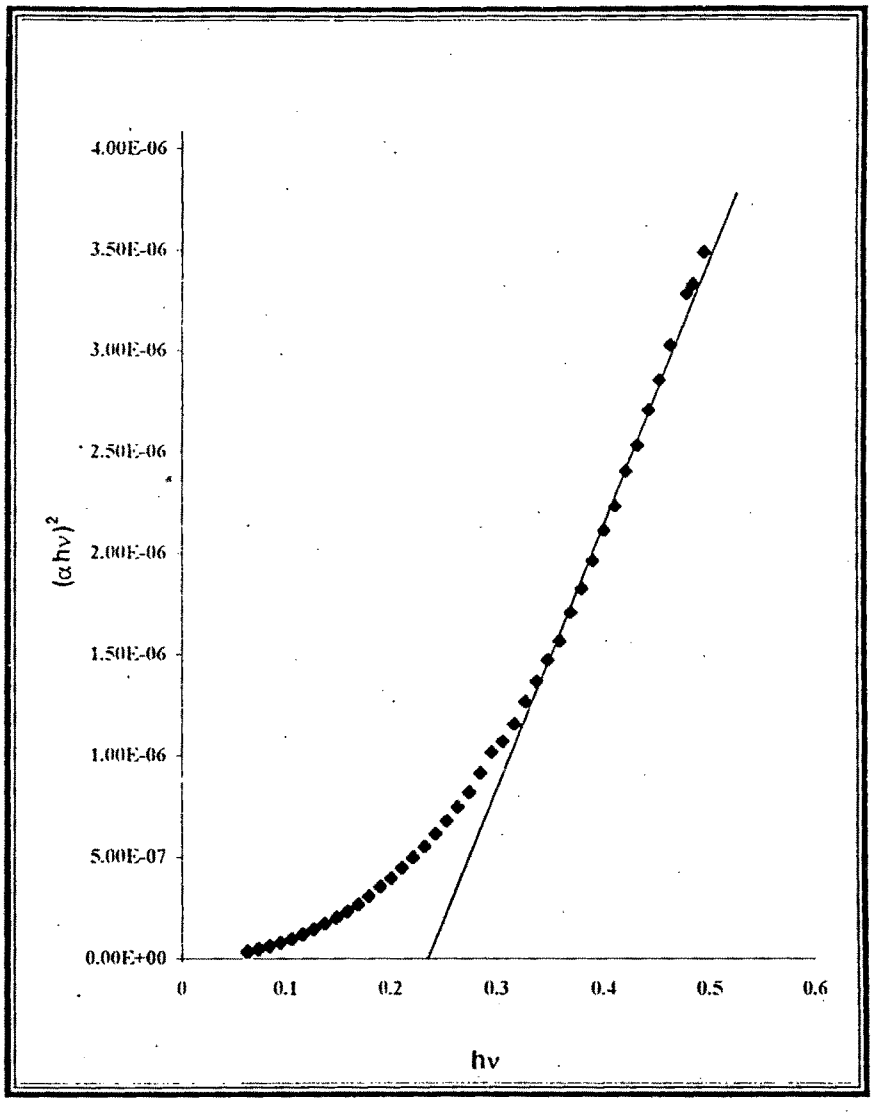

Fig. 15(c)

$InBi_{0.8}Sb_{0.2}$

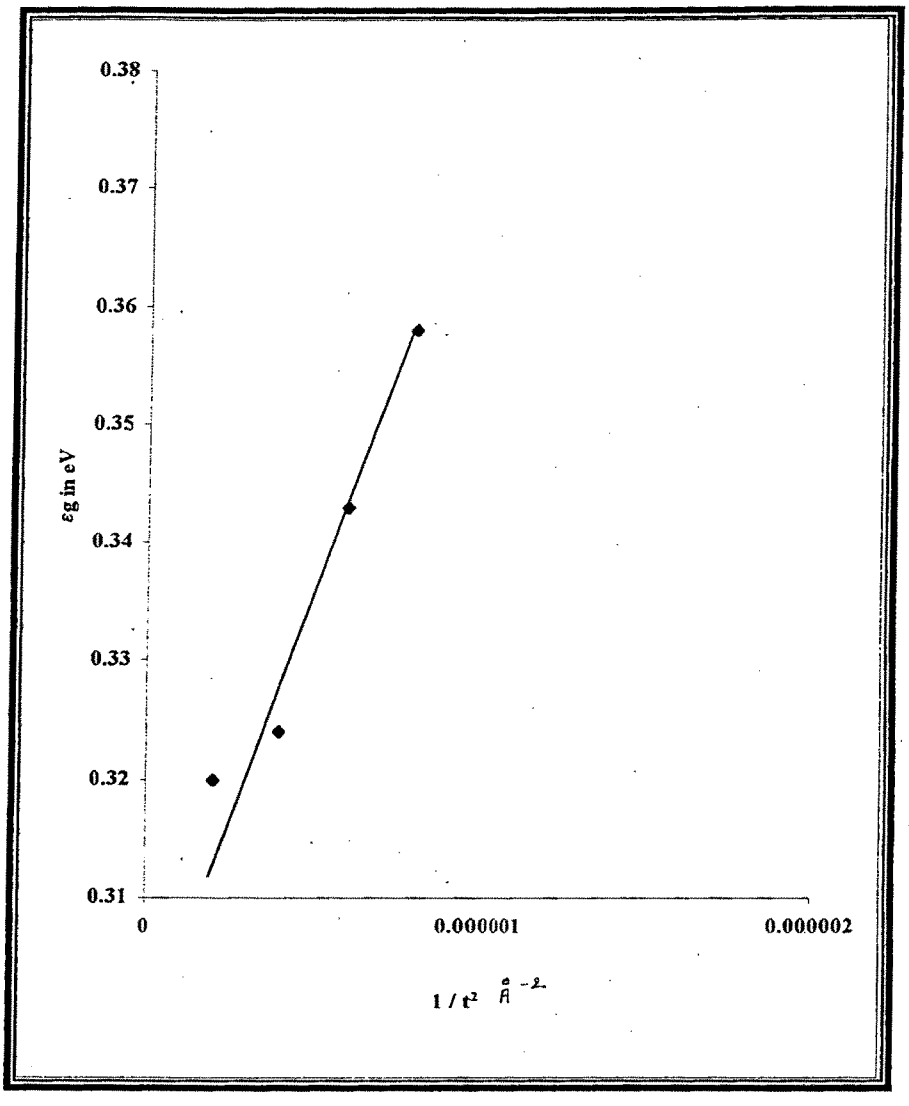

Fig. 16(a)

$InBi_{0.8}Se_{0.2}$

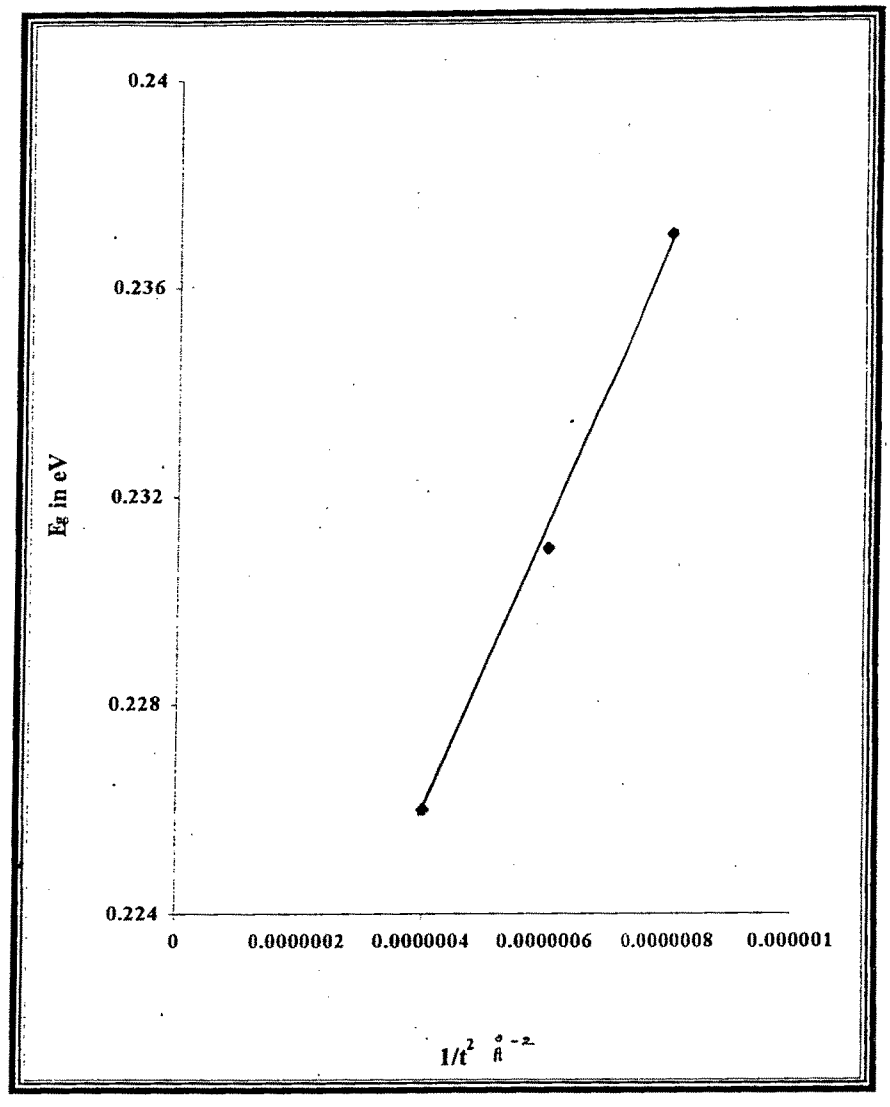

Fig. 16(b)

band are separated by an additional amount of ΔE[30]. In the thin film specimens, provided smearing of energy levels by temperature and diffuse scattering of the carriers at the film surfaces are not significant, this shift will increase the band gap and affect the optical behavior of semiconducting films. The absorption is reduced in thinner films as compared with the bulk. ΔE is given by

$$\Delta E = \frac{h^2}{8m^*t^2} \quad \text{or} \quad \frac{h^2p^2}{2m^*}\frac{1}{t^2}$$

Here m* is the effective mass of the charge carrier, t = thickness of the film, ΔE is the K.E contribution due to motion normal to the film plane and h = Planck's constant.

The plots of Eg versus $1/t^2$ for $InBi_{0.8}Sb_{0.2}$ and $InBi_{0.8}Se_{0.2}$ given in Fig- 16 (a) and (b) are in agreement with the above relation and imply the quantum size effect operative in the present case.

It is also known that a fairly large number of dislocations are created during the formation of the thin films and their density increases as the thickness increases up to a particular thickness beyond which the density is practically constant. However, the dependence of dislocation density on thickness has not been quantified and in any case the dependence is complex. There are considerable lattice disturbances due to dislocations, viz., the local stress fields around a dislocation, disrupted or dangling bond with its specific charge and the space charge domain that

forms immediately in semiconductors. The compression and dilation in strain patterns brought about by edge dislocations have an effect in changing the forbidden gap of the semiconductor. This is because of resulting local compression increment in the deformation potential relation. Another influence is due to dangling bond resulting in an energy level within the forbidden gap.

With the increase in film thickness, the effect of the initial granular structure on the optical properties decreases but is not eliminated completely. Therefore, thickness dependence is still observed although the general behavior of the optical parameter, i.e. band gap , follows that of the bulk, at least qualitatively. For a very thick crystal, (i.e., ideally infinite thickness) the electron energy is a multi valued continuous function of the quasimomentum. The variation of band gap with the crystallite size has been explained by the modified form of Steller's formula[39]. According to him the increased barrier height is given by

$$E = E_0 + C\,(X - f\,D)^2 \quad \ldots\ldots\ldots\ldots\ldots (11)$$

where, C = term depending on density of charge carriers, electronic charge and dielectric constant of the material

E_0 = original barrier height

X = barrier width

D = grain dimension

f = factor depending on the charge accumulation and carrier concentration.

From literature, it is known that the grain size is approximately proportional to the thickness. Hence grain size increases due to the increase in thickness of the film[18]. So, if we replace D, the grain size in the above equation by the film thickness t, E should be proportional to $(X - f t)^2$.

In the present observations we find that the band gap varies inversely as the square of the film thickness. Hence it can be concluded that the observed band gap variation with thickness cannot be attributed to the above effect. Thus in these InBi: Sb and Se films the quantum size effect is dominant, (explaining the band gap dependence on film thickness) rather than the effect produced by the dislocation density variation.[15]

Band gap variation with composition:

For this study, thin films of $InBi_{1-x}Sb_x$ and $InBi_{1-x}Se_x$ were obtained with x = 0.2, 0.3, 0.4 using thermal deposition on NaCl crystal substrates. The film thickness was kept constant at 1250 Å for $InBi_{1-x}Sb_x$ and at 1275 Å for $InBi_{1-x}Se_x$. The IR spectra of the films were obtained using FTIR spectrophotometer as described earlier. From the absorbance versus wave number curves the quantity $(\alpha h\nu)^2$ as a function of $h\nu$ was

calculated. Here α is absorption coefficient and hν is the photon energy.

The plots of $(\alpha h\nu)^2$ versus hν are shown in Fig.17(a) and (b) Fig.18 (a) and (b) for $InBi_{1-x}$ Sb_x and $InBi_{1-x}$ Se_x, respectively, with x = 0.3 and 0.4. Similar plots for x = 0.2 for both types of films have already been shown in Fig 14 (a) and 15 (a). It can be seen that the plots are linear in the high absorption side of the curves. The extrapolation of these linear parts to the zero of abscissa has also been shown in the figures. The intercepts of these extrapolations on the hν axis yield the band gaps which are seen to depend on the x value as illustrated by the plots of Eg versus x in Fig. 19 and Fig. 20 and for the two cases. As can be seen the band gap decreases with decrease in x, nearly linearly. Similar dependence in the case of other III - V compounds such as InAs, GeAs, INSb and AlSb has been reported by earlier workers[32].

It is important to note that whereas InBi is semi metallic, $InBi_{1-x}Sb_x$ and $InBi_{1-x}$ Se_x (x = 0.2, 0.3, 0.4) have been found to be semi conducting, as implied by the finite band gaps obtained for these two materials. This fact is also supported by the resistivity - temperature results as described earlier. However the most significant observation that can be drawn is that by varying the Sb/Se content in the material the band gap can be varied. For IR detection at 8 to 10 micron wavelength the required band gap is about 0.1 eV. While modification of band gap of InSb from 0.16 eV to lower values has not been successful, the approach

$InBi_{0.7}Sb_{0.3}$ (1250 Å)

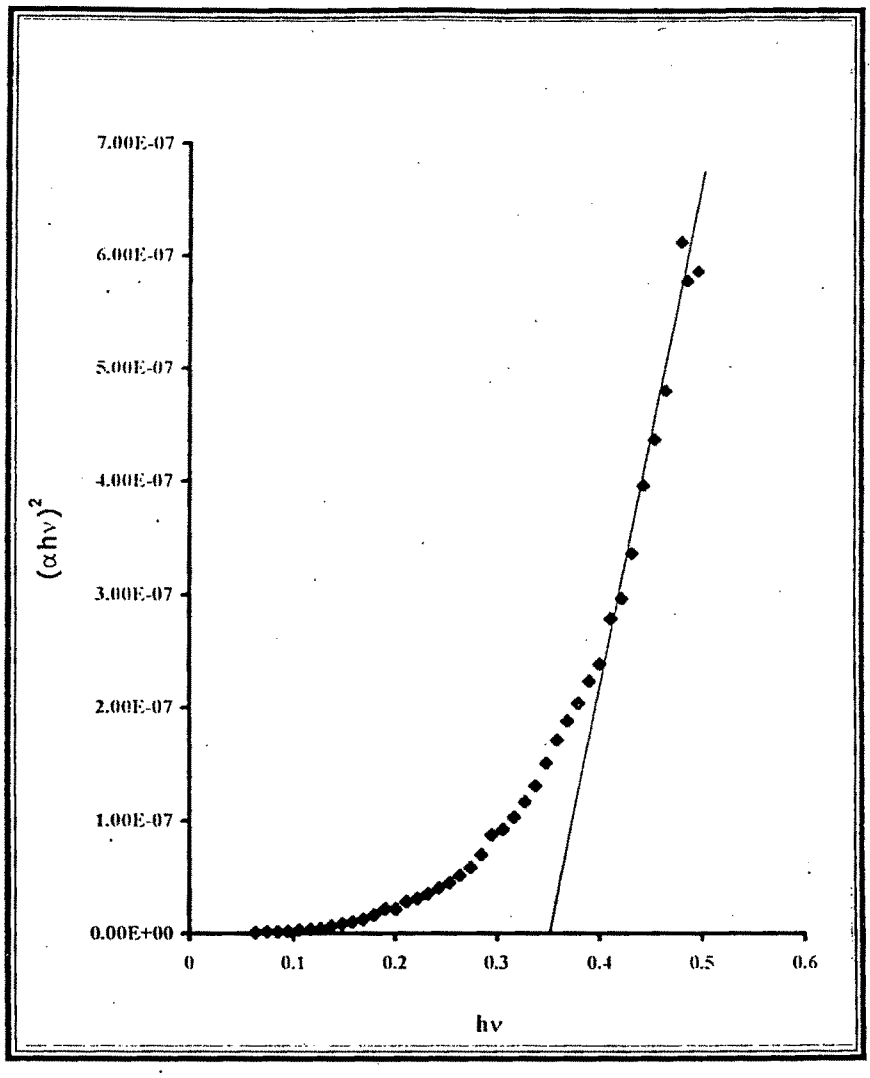

Fig. 17(a)

$InBi_{0.6}Sb_{0.4}$ (1250Å)

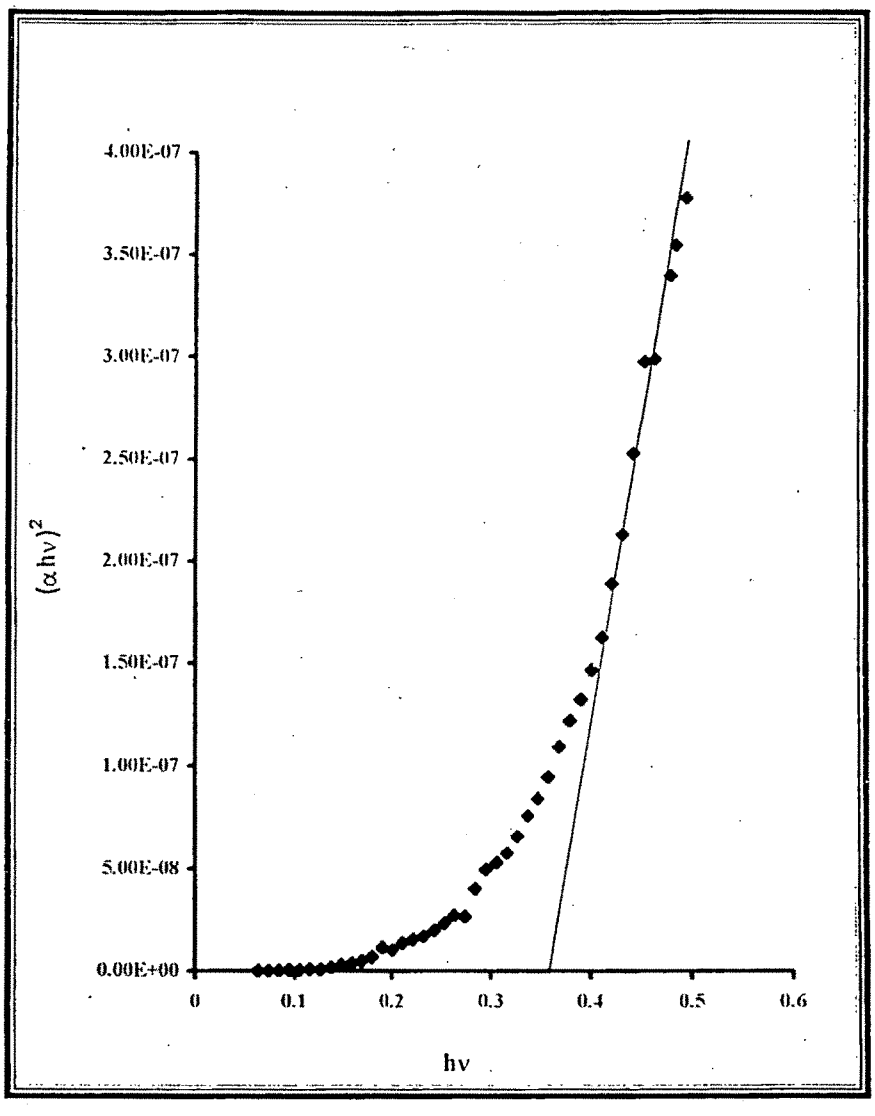

Fig. 17(b)

$InBi_{0.7}Se_{0.3}$ (1275Å)

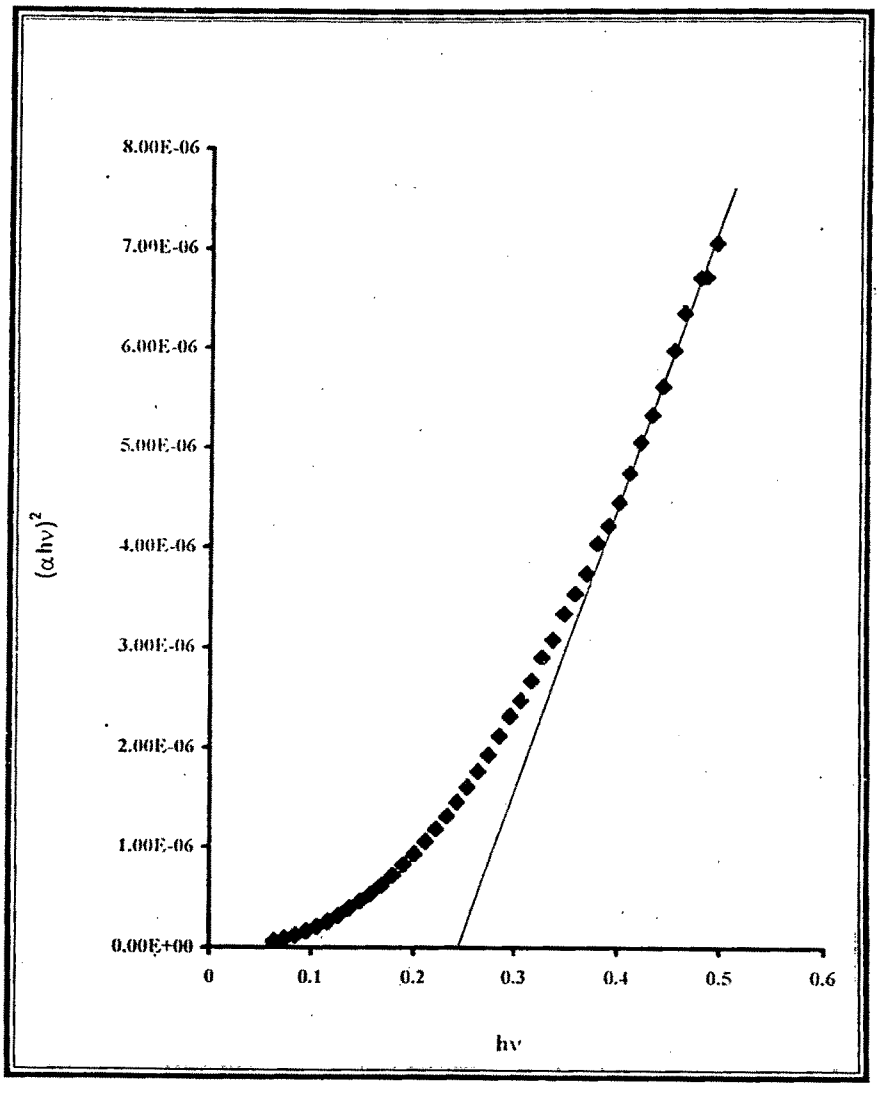

Fig. 18(a)

$InBi_{0.6}Se_{0.4}$ (1275Å)

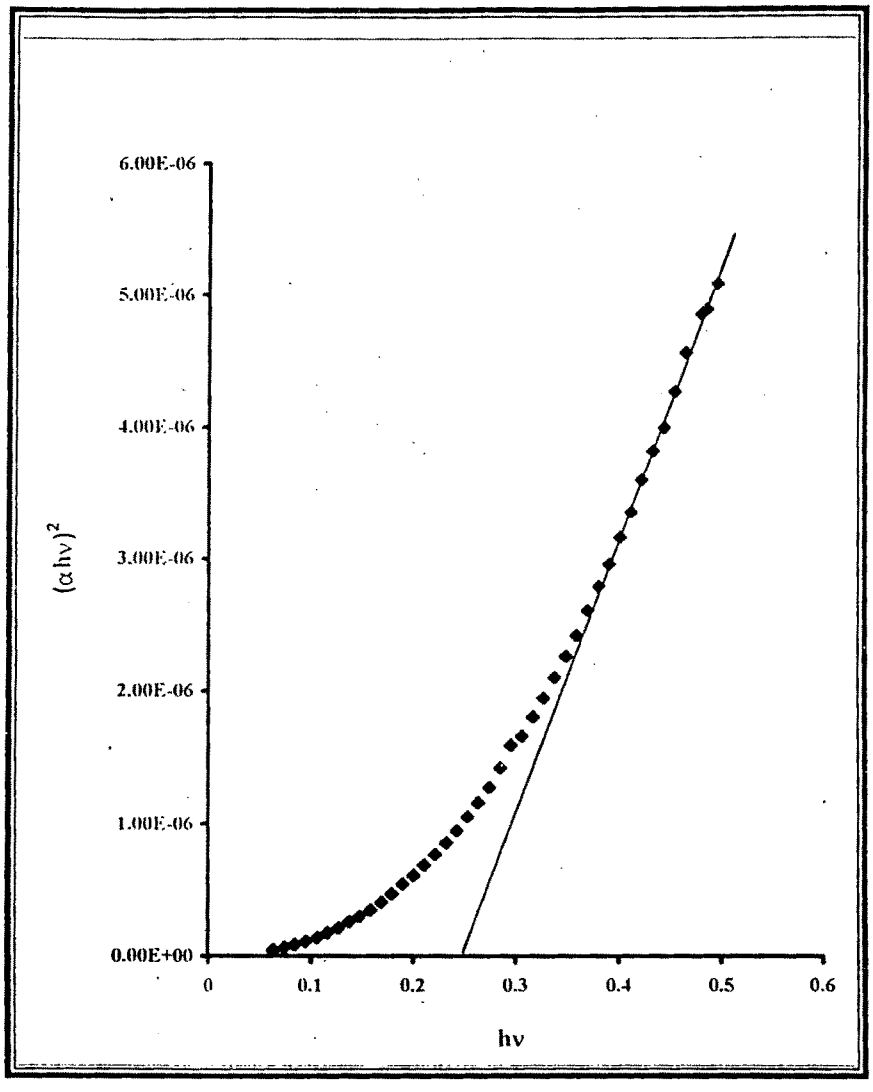

Fig. 18(b)

$InBi_{1-x}Sb_x$ (1250Å)

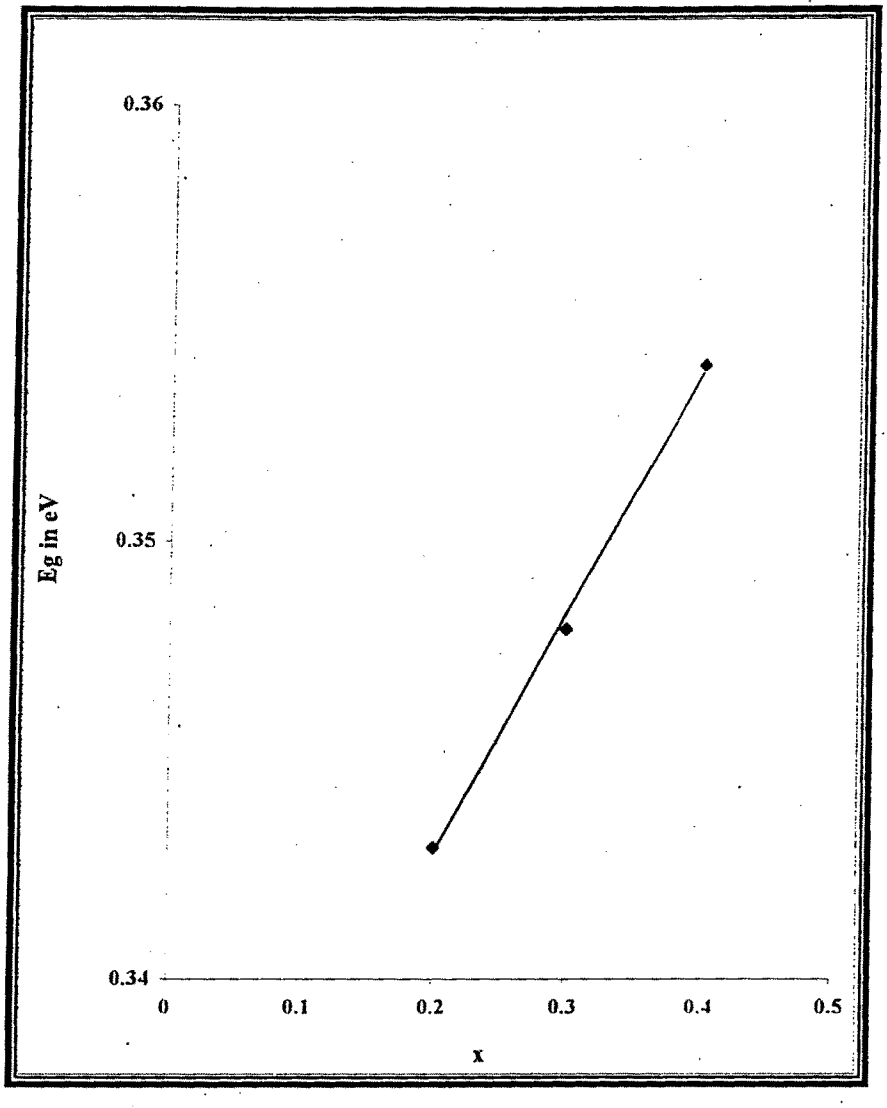

Fig.19

$InBi_{1-x}Se_x$ (1275Å)

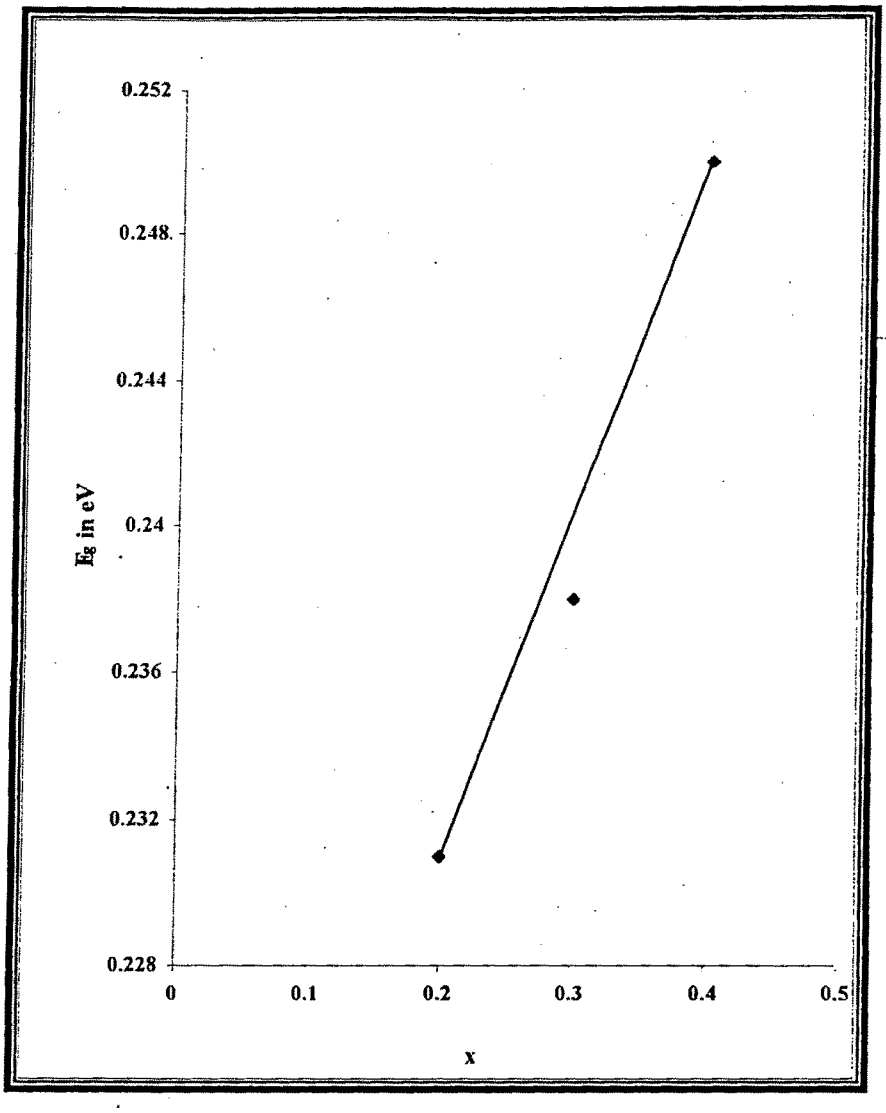

Fig. 20

of converting a semi - metal to a semi conductor by using suitable dopant and its concentration may prove useful. In this regard in the present case further reducing Sb/Se in InBi may lead to a band gap value around 0.10 eV.

CONCLUSIONS :

(1) The resistivity of $InBi_{1-x}Sb_x$ and $InBi_{1-x}Se_x$ thin films has been found to decrease with increasing film thickness approaching bulk value.

(2) The resistivity activation energy does not show any significant variation with variation in film thickness.

(3) The optical band gap of $InBi_{1-x}Sb_x$ and $InBi_{1-x}Se_x$ is found to increase with increase in x both in the cases of crystals and thin films.

(4) The optical band gap of the thin films has been found to vary as inverse square of film thickness implying quantum size effect operative for thicknesses upto about 1500Å to 2000Å.

REFERENCE

1. Dr. S. Mohan, Electrical Properties of thin films – Measuring Techniques "Lecture note on Introduction to thin film technology" Feb / Sep. 1983, regional Instrumentation Centre, I.I.Sc. Banglore
2. Goswami A. and Ojna S.M., Thin Solid Film, 16 (1973) 187
3. Alder R.B., Smith A.C., Ligini R.L., Introduction to Semiconductor Phys., Eastern Pvt. Ltd., new Delhi., (1973)
4. Petritze, Phys. Rev. 104 (1956) 1508
5. D.V. Krishna Sastri and P. Jayarama Reddy, Thin Solid Films (1983) 139
6. D.V. Krishna Sastri and P. Jayarama Reddy, Phys. Stat. Sol. (a) 58 (1980) 213
7. Subbarao T. and Chaudhari A.K., J. Phys.(D) Appl. Phys., 19 (1986) 861
8. Van Vechatan, J.A. (1969) Phys. Rev. 182, 801
9. Wemple, S.H. and Didomenico, M. (1971) phys. Rev. 133, 1338
10. Streetman B.G. Solid State Electronic Devices, Prentic Hall of Indian Pvt., New Delhi (1982)
11. Heavens O.S., Optical properties of Thin Solid Films, Butterworths, London (1955)
12. Heavens O.S., Rept. Progr. Physics, 23 (1960) 1

13. Bering P.H., Physics of Thin films, Academic Press NY (1964) 69

14. Bernnett H.E. and Bennettin J.M., Physics Of Thin Films, Academic Press NY 4 (1967)1

15. Sze S.M., Physics of Semiconductor Devices, Wiley Eastern Ltd., New Delhi (1979)

16. Bhatt V.P. Gireesan K., Desai C.F., Cryst. Res. Technol., 25 (1990) 209

17. Dang Tran Quan, Thin Solid Films, 149 (1987) 197

18. Bhatt V.P. Gireesan K., Desai C.F., Cryst. Res. Technol., 24 (1989) 187

19. Barden J., Hall H., and Bhatt F.J., Proc. Of The Conf. On Photoconductivity, NY (1956) 146

20. Tovar Barradas R., Rincon C., Genzalez j. and Sancher Pertez G., J. Phys. Chem. Solids 45 (1984) 1185

21. Eva C., Freeman and Willam Paul, Phys. Rev., (B) 20 (1979) 716

22. Mendolia J. and Lemone D., Phys. State Solid. (a) 97 (1986) 601

23. Bube R.H., photoconductivity of Solids, John Wiley and Sons Inc., NY (London) (1960)

24. Sizov F.F., Acta Phys. Pol. (A) (Poland) 79 1 (1991) 83 – 96

25. Bauer S., Am. J. Phys. (USA) 60 3 (1992) 257

26. Bryja., Jezierki K., Misiewicz J., Thin Solid Films (Switzrland) 229 1 (1993) 11

27. Pal Gayatri, Sebastian K.C., Chavda N.D., Desai C.F., Chintalapudi S.N., Somayajulu D.R.S. Electric Field Gradients in pure Te and Se doped InBi Systems, DAE – Solid State Symposium, Vol. – 40C, 240 (1997)

28. Stasenko A.K., Sov. Phys. Solid State, 10 (1968) 186

29. Damodardas V. and Karunakaran D., J. Appl. Phys., 54 (1983) 5252

30. Chopra K.L., Thin Film Phenomena, MeGraw Hill NY (1969)

31. Pankove J.I., Optical Process in Semiconductors Preventic – Hall Inc., NY (1971) 103

32. Semiconductors and Semimetals Ed, Willardson R.K. and Beer A.C., 1 [Academic Press, NY] (1966) 143 – 156

Cryst. Res. Technol.	33	1998	5	733–736

PANDYA, G. R., DESAI, C. F., SHAH, R. C., SHAH, K. R.

Physics Department, Faculty of Science, M.S. University of Baroda, Baroda-390002

Growth and Dislocation Etching of $InBi_{0.8}Sb_{0.2}$ Single Crystal

$InBi_{0.8}Sb_{0.2}$ single crystals have been grown by zone melting method. The freezing interface temperature gradient of 30 °C/cm has been found to yield the best quality crystals obtainable at growth velocity 1.0 cm/hr. Traingular features have been obtained on the free surface of the as grown crystal. A new dislocation etchant based on nitric acid has been found to give reproducible etch-pitting on the cleavage surface. Standard tests for a dislocation etchant have been carried out and results are reported.

InBi has a tetragonal structure with $c/a = 0.955$ and space group P4/nmm (BINNIE. W. P., CHUNG, D. Y., SAUNDERS, G. A., SAVAGE, C.). Although it is not a semiconductor like the other III–V compounds, its low melting point (109.5 °C) and easy cleavage makes it attractive for basic studies. However, the crystal is quite soft (BHATT, DESAI). InBi crystals have been grown by various methods like Bridgman, Czochralski and zone-melting by various workers. Studies on disclocation etching and features on as-grown crystal surfaces have also been reported (PANDYA and VYAS; THORSEN, BERLINCOURT; ROY and GLASSCO; ASANABE; WALTER; FISCHLER; SHAPIRA, Y., WILLIAMSON, S. J., FISCHLER. S.; BHATT and DESAI). The electrical and mechanical properties have been reported by some of these workers. The crystal has been shown to exhibit marginally metallic conductivity. With an intention to study effects of an impurity on crystal growth, perfection and hardness of the crystal, the present work had been undertaken.

InSb, like InBi, is a III–V compound but its properties very significantly differ from those of InBi. The lattice of InBi is close to cubic type with regard to the unit cell parameters. Therefore Sb can expectedly substitute Bi in the InBi lattice. Therefore Sb has been added to study its effect on crystal growth, crystal perfection and hardness of InBi. We report here, crystal growth and dislocation etching of $InBi_{0.8}Sb_{0.2}$.

The stoichiometric weight proportions of the elemental materials of 5N purity were mixed and melted under a pressure of 10^{-5} torr in a sealed quartz ampoule. For this, the melt was continuously stirred for 24 hr and then air quenched. The ingot so prepared was subjected to growth by zone-melting. Prior to growth, it was zone-levelled by eight alternate zone passes. The growth velocity was 1 cm/hr and the freezing interface temperature gradient was maintained at 30 °C/cm by controlling the furnace temperature within ±1 °C. The maximum zone temperature was kept 50 °C above the melting point (128 °C).

The X-ray diffractogram of powdered samples from the crystal exhibited peaks corresponding to InBi, InSb and Sb. The free surface of the as grown crystal was frequently

Fig. 1. Terraced triangular features on the free surface of the crystal

observed to have triangular terraced features. The triangles are nearly equilateral. The InBi structure being nearly that of cubic type, these features bounded by triangles imply the observation surface to be of (111) orientation. Hence, planes of {111} type may be responsible to develop growth fronts resulting in to these features (Fig. 1).

This is typical of the layer growth mechanism. Crystals obtained were cleaved and the cleavage plane (001), was observed to be quite plane and mirror like, nearly as in the case of InBi crystals.

Various workers (BHATT, DESAI; WALTER; ROY, GLASSCO) have reported dislocation etchants for InBi single crystals. These etchants could not produce successful results due

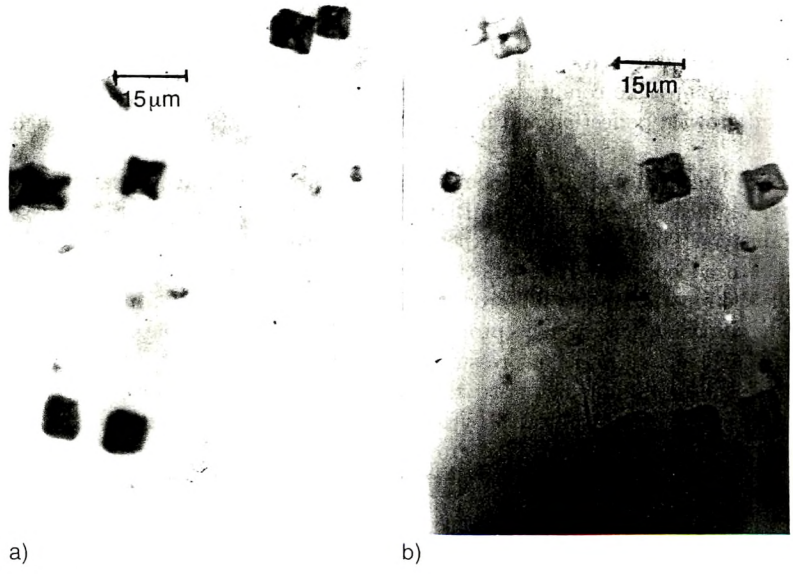

Fig. 2. Etch pits on oppositely matched cleavage faces

to the presence of antimony in the crystals. Although the surface has an exceptionally low tendency to oxidize in air, it has an equally high tendency to corrode under chemical reactions.

After numerous trials, a dislocation etchant has been developed to work on (001) of the crystals. The etchant consists of 1 part saturated solution of citric acid +1.0 part conc. HNO_3 (70%) and 10 part water. One part of this solution was then added to 20 parts of glacial acetic acid. This mixture was used to etch the cleavage plane of freshly cleaved crystals. The minimum etching time to produce well defined point-bottomed square pits at room temperature was about 40 sec and this could be extended upto 85 sec. The etching was followed by rinsing the etched specimens in double distilled water and then the specimens were air-dried. The square shape of pits corresponds with the four-fold axis [001].

Etch patterns obtained on oppositely matched cleavage faces are shown in Fig. 2.

There is almost one to one correspondence of etch pits observed, implying that the etch pits are necessarily at dislocation sites.

Fig. 3 shows a triaxial boundary delineated by the etch pits.

The etch pit density n along the three boundaries obeys the relation $n_1 = n_2 - n_3$, where the branches are numbered as shown in Fig. 3 (WERNICK, J. H., HOBSTETTER, J. N., LOVELL, C. and DORSI, D.). Further tests for dislocation etchant, like successive etching of surface, scratching or indenting the surface and etching it, were conducted to yield satisfactory results.

Thus the etchant composition stated above is capable of revealing grown-in and freshly produced dislocations intersecting the cleavage plane. The average dislocation density of the crystals, measured by etch-pit count method on (001), was found to be of 10^4 cm^{-2} order.

Fig. 3. Triaxial boundary delineated by the etch pits

References

ASANABE, S.: Mem. Faculty of Science $\mathbf{B_2}$ (2) (1956) 82
BHATT, V. P., DESAI, C. F . Bull Material Sci. **4** (1982) 23
BINNIE, W. P.: Acta Crystal **9** (1956) 686
CHUNG, D. Y., SAUNDERS, G A., SAVAGE, C . Phys. Lett. **47A** (1974) 449
FISCHLER, S.: TMS, AIME **230** (1964) 340
PANDYA, G R , VYAS, S M.: Cryst Res. Technol **28** (2) (1993) 163
ROY, U., GLASSCO, D.: J. Cryst. Growth **16** (1972) 227
SHAPIRA, Y., WILLIAMSON, S. J., FISCHLER, S. Phys. Rev **144** (1966) 715
THORSEN. A C., BERLINCOURT, T. G · Nature (Landon) **192** (1961) 959
WALTER, H. U.. J Cryst. Growth **19** (1973) 351
WERNICK, J H , HOBSTETTER J. N , LOVELL, L C , DORSI, D J Appl Phys **29** (1958) 1101

(Received September 26, 1997: Accepted January 5. 1998)

Proc. Intl. Workshop Prep. & Charact. Tech. Imp. Single Crystals
National Physical Laboratory, New Delhi, Feb. 26-28, 2001
S K. Gupta, S.K. Halder and G. Bhagavannarayana (Eds.)

GROWTH OF $InBi_{1-x}Sb_x$ SINGLE CRYSTALS GROWN BY SYRINGE PULLING METHOD

G. R. Pandya, K.R. Shah, S. M. Vyas, C.F. Desai

Physics Department, Faculty of Science,
The M. S. University Of Baroda,
Vadodara, Gujarat, India.

$InBi_{1-x}Sb_x$ single crystals have been grown by syringe pulling method In this method melt was allowed to cool freely to room temperature, which took about 10 minute Crystals were cleaved along the cleavage plane, parallel to the vertical growath axis Here, the stainless steel needle work as the heat sink. Presumably, the crystal structure that of the parent InBi tetragonal type and cleavage plane (001) face After numerous trial the author's have developed a new dislocation etchant, which is capable of revealing dislocations intersecting the cleavage plane is also reported

INTRODUCTION

For metals and alloys the methods of crystal growth from melt like Bridgman and zone-melting techniques have been widely used for obtaining the large sized crystals. For InBi single crystals growth such methods have been used by different authors [1-5]. This intermetallic compound belonging to the tetragonal system with the c/a =0.955 with a very low melting point of 109.5 ^{0}C. Present paper reports use of the syringe pulling method for the growth of single crystals of $InBi_{0.8}Sb_{0.2}$ which is describe below.

Indium , Bismuth and Antimony of 5N purity, were used for preparation of the charge These were weighed to stoichiometric proportions and sealed under the vacuum order of 10^{-4} Pa in a quartz ampoule of 1.0 cm in diameter and 15cm in length. Which was placed in alloy mixing furnace at a 50 ^{0}C higher temperature and charge was cooled to room temperature. The solidified charge was kept in the form of small grannuals was transferred to a porcelain crucible. This was then kept over the burner flame for melting. A corning glass of syringe of 5-ml capacity was kept vertically on a stand beside the burner When the charge was melt at a temperature reach around 150 ^{0}C , the oxide layer formed on the surface of the molten charge was scraped out and simultaneously the syringe mouth was placed into the molten charge was sucked within 30 Sec. Followed by quick attachment of a stainless steel needle. Then the charge was allowed to cool freely to room temperature, which take time about 10 min. The syringe was then broken and crystal taken out. The cylindrical surface had a bright shining . The crystal was then cleaved at an ice temperature. Here in this method, the needle worked as a heat sink and site of nucleation. The rest of the syringe system, being non-conducting, effects uni-directional solidification [6]. A typical as grown crystal is shown in fig.1.

As shown in fig.2(a) and 2(b) the surface are quite plane with a few cleavage lines which also exhibit one to one correspondence across the pair of counter parts. Thus the perfectness of the crystals were found. The average dislocation density was found to be about 10^4 cm^{-2}, measured by the etch pit count method using the dislocation etchant established by the authors Thus the syringe pulling method is quick and as successful as the zone melting method Also the new etchant is capable of revealing dislocation intersecting the cleavage plane

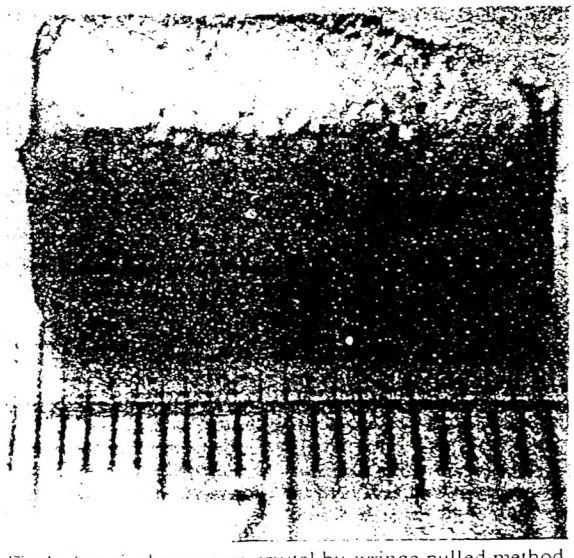

Fig.1: A typical as-grown crystal by syringe pulled method.

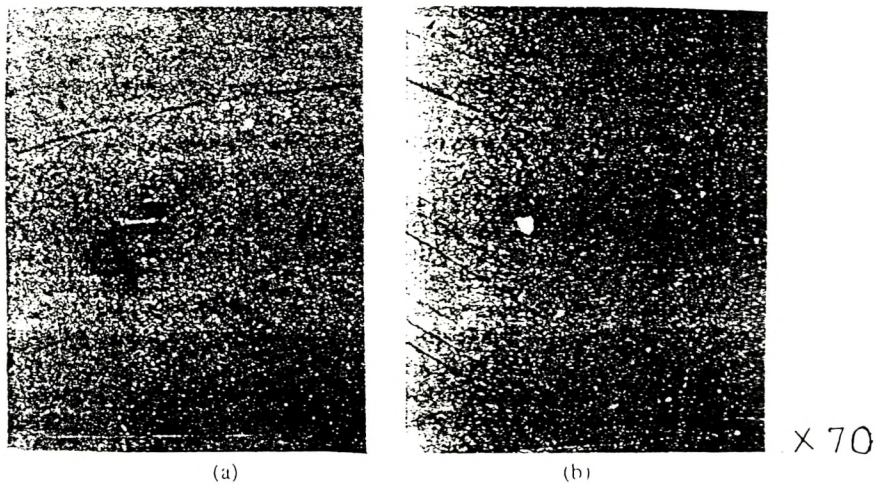

Fig.2: The counter parts of cleaved surfaces of the crystal.

After numerous trials a new dislocation etchant has been developed to work on cleavage plane (001) syringe pulled crystals. The etchant consist of 1 part solution of "A" and 20 part of glacial acetic acid. The solution "A" consisting of one part saturated solution of citric acid + 1 part of HNO_3 (70%) and 10 part of distilled water. The etchant was used to etch the freshly cleaved crystal face, the minimum etching time 40 Sec. Required to produced well defined point bottomed square pits at room temperature.

The sample shown in fig 3(a) was etched for 40 Sec. And the same sample was further etched for 90 Sec. The etch pattern obtaining in fig 3(b), as can be seen that the etch pits have increased in size with the increased etching time.

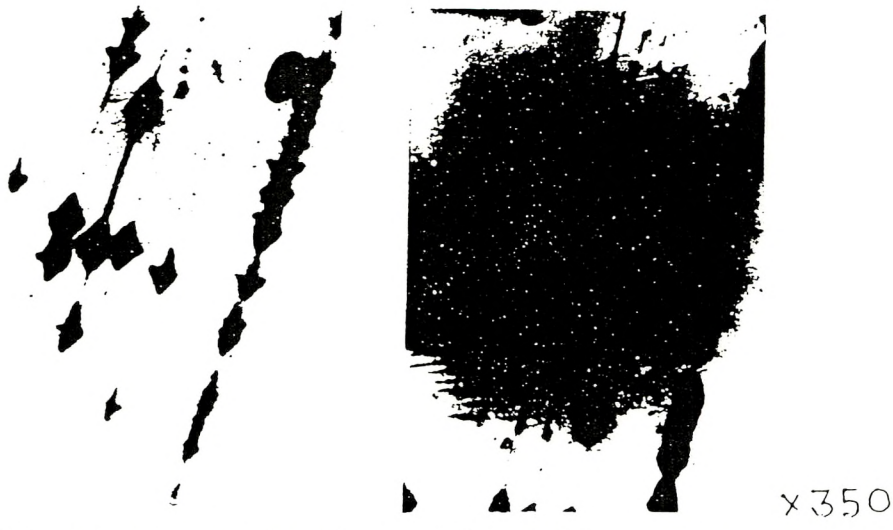

Fig. 3(a) &(b): Etch patterns observed on oppositely matched cleavage counter parts.

Thus it concluded that the syringe pulling method is quite quick and convenient method for crystals with preferred orientation and better perfection.

ACKNOWLEDGEMENT

The authors are grateful to the UGC, New Delhi for financial support for the work under DRS programme.

REFERENCES:

1. Bhatt V. P., Desai C.F. : Ind. J. Pure Appl . Phys. **16**, 960 (1978)
2. Fischler , S. : TMS-AIME **230**, 340 (1964).
3. Jani T. M. , Pandya G.R. , Desai C. F. : Cryst. Res. Technol. **28 (5)**, k40 (1993)
4. Pandya G. R. , Vyas S. M. : Cryst. Res. Technol. **28,** 163 (1993)
5. Satio Y. : J. Phys. Soc. Jap. **17,** 716 (1962)
6. Jani T. M. , Pandya G.R. , Desai C. F. : Cryst. Res. Technol. **28 (6)**, k57 (1993)